

Journal Pre-proof

Design, synthesis and discovery of 2(1H)-quinolone derivatives for the treatment of pulmonary fibrosis through inhibition of TGF- β /smad dependent and independent pathway

Linlin Xue, Dexin Deng, Shoujun Zheng, Minghai Tang, Zhuang Yang, Heying Pei, Yong Chen, Tao Yang, Kongjun Liu, Haoyu Ye, Lijuan Chen

PII: S0223-5234(20)30226-9

DOI: <https://doi.org/10.1016/j.ejmech.2020.112259>

Reference: EJMECH 112259

To appear in: *European Journal of Medicinal Chemistry*

Received Date: 21 January 2020

Revised Date: 18 March 2020

Accepted Date: 18 March 2020

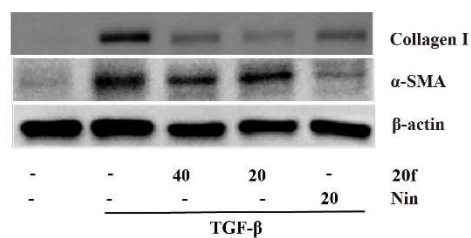
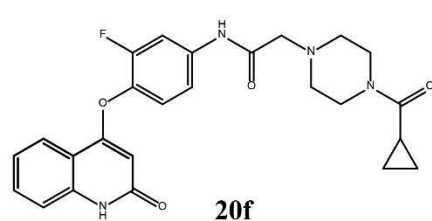


Please cite this article as: L. Xue, D. Deng, S. Zheng, M. Tang, Z. Yang, H. Pei, Y. Chen, T. Yang, K. Liu, H. Ye, L. Chen, Design, synthesis and discovery of 2(1H)-quinolone derivatives for the treatment of pulmonary fibrosis through inhibition of TGF- β /smad dependent and independent pathway, *European Journal of Medicinal Chemistry* (2020), doi: <https://doi.org/10.1016/j.ejmech.2020.112259>.

This is a PDF file of an article that has undergone enhancements after acceptance, such as the addition of a cover page and metadata, and formatting for readability, but it is not yet the definitive version of record. This version will undergo additional copyediting, typesetting and review before it is published in its final form, but we are providing this version to give early visibility of the article. Please note that, during the production process, errors may be discovered which could affect the content, and all legal disclaimers that apply to the journal pertain.

© 2020 Published by Elsevier Masson SAS.

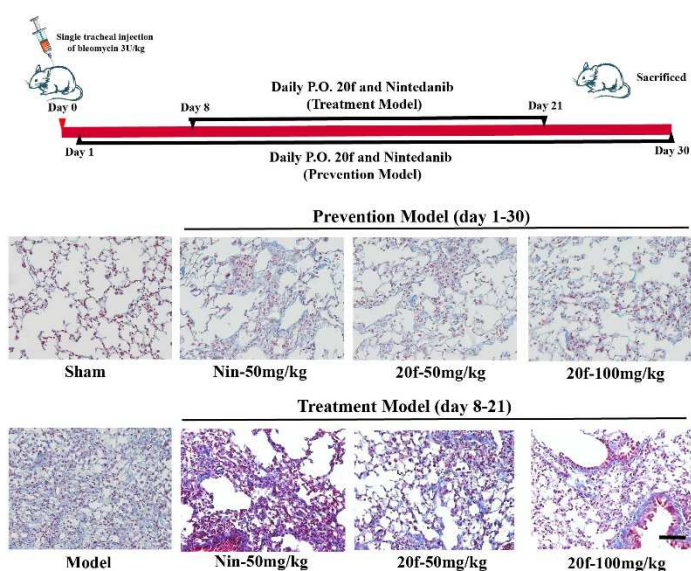
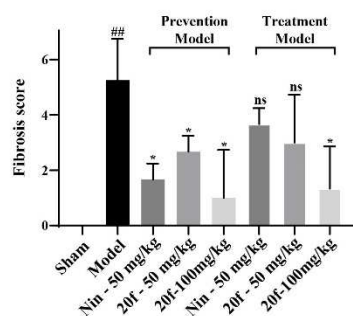
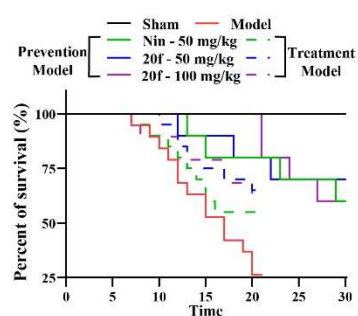
Graphical abstract



Collagen deposition

Fibroblasts migration

TGF-β/Smad dependent and independent pathways



Design, synthesis and discovery of 2(1H)-quinolone derivatives for the treatment of pulmonary fibrosis through inhibition of TGF- β /Smad dependent and independent pathway

Linlin Xue¹, Dexin Deng¹, Shoujun Zheng, Minghai Tang, Zhuang Yang, Heying Pei, Yong Chen, Tao Yang, Kongjun Liu, Haoyu Ye^{*}, Lijuan Chen^{*}

State Key Laboratory of Biotherapy and Cancer Center, West China Hospital, Sichuan University and Collaborative Innovation Center, Chengdu, 610041, China

^{*} Corresponding authors. Lab of Natural Product Drugs, Cancer Center, West China Medical School, West China Hospital, Sichuan University, Chengdu 610041, PR China.

E-mail addresses: haoyu_ye@scu.edu.cn (H. Ye), chenlijuan125@163.com (L. Chen).

¹ Both authors contributed equally to this study.

ABSTRACT:

Idiopathic pulmonary fibrosis (IPF) is a progressive, life-threatening and interstitial lung disease with the median survival of only 3 to 5 years. However, due to the unclear etiology and problems in accurate diagnosis, up to now only two drugs were approved by FDA for the treatment of IPF and their outcome responses are limited. Numerous studies have shown that TGF- β is the most important cytokine in the development of pulmonary fibrosis and plays a role through its downstream

signaling molecule TGF-binding receptor Smads protein. In this paper, compounds bearing 2(1H)-quinolone scaffold were designed and their anti-fibrosis effects were evaluated. Of these compounds, **20f** was identified as the most active one and could inhibit TGF- β -induced collagen deposition of NRK-49F cells and mouse fibroblasts migration with comparable activity and lower cytotoxicity than nintedanib *in vitro*. Further mechanism studies indicated that **20f** reduced the expression of fibrogenic phenotypic protein α -SMA and collagen \square by inhibiting the TGF- β /Smad dependent pathways and ERK1/2 and p38 pathways. Moreover, compared with the nintedanib, **20f** (100 mg/kg/day, p.o) more effectively alleviated collagen deposition in lung tissue and delayed the destruction of lung tissue structure both in bleomycin-induced prevention and treatment mice pulmonary fibrosis models. The immunohistochemical experiments further showed that **20f** could block the expression level of phosphorylated Smad3 in the lung tissue cells, which resulted in its anti-fibrosis effects *in vivo*. In addition, **20f** demonstrated good bioavailability (F = 41.55% vs 12%, compare with nintedanib) and an appropriate elimination half-life ($T_{1/2}$ = 3.5 h), suggesting that **20f** may be a potential drug candidate for the treatment of pulmonary fibrosis.

Keywords:

Pulmonary fibrosis; Collagen accumulation; Bioisosteres; TGF- β /Smad pathway; Anti-fibrosis effects.

1. Introduction

Idiopathic pulmonary fibrosis (IPF) is the most common idiopathic interstitial pneumonia [1]. Like other interstitial lung diseases, the characteristic of idiopathic pulmonary fibrosis is progressive scarring or fibrosis that is distributed and deposited between the interstitial spaces of the lungs [2-3], hindering normal gas exchange and decreased lung capacity and leading to clinical symptoms such as unexplained exertional dyspnea, chronic dry cough, or Velcro like crackles on examination with the median survival time of three to five years from diagnosis [4]. Although the pathogenesis of IPF has not been elucidated, it is generally believed that early stage is pneumonia and lung injury, and the late stage is the deposition of extracellular matrix (collagen fiber).

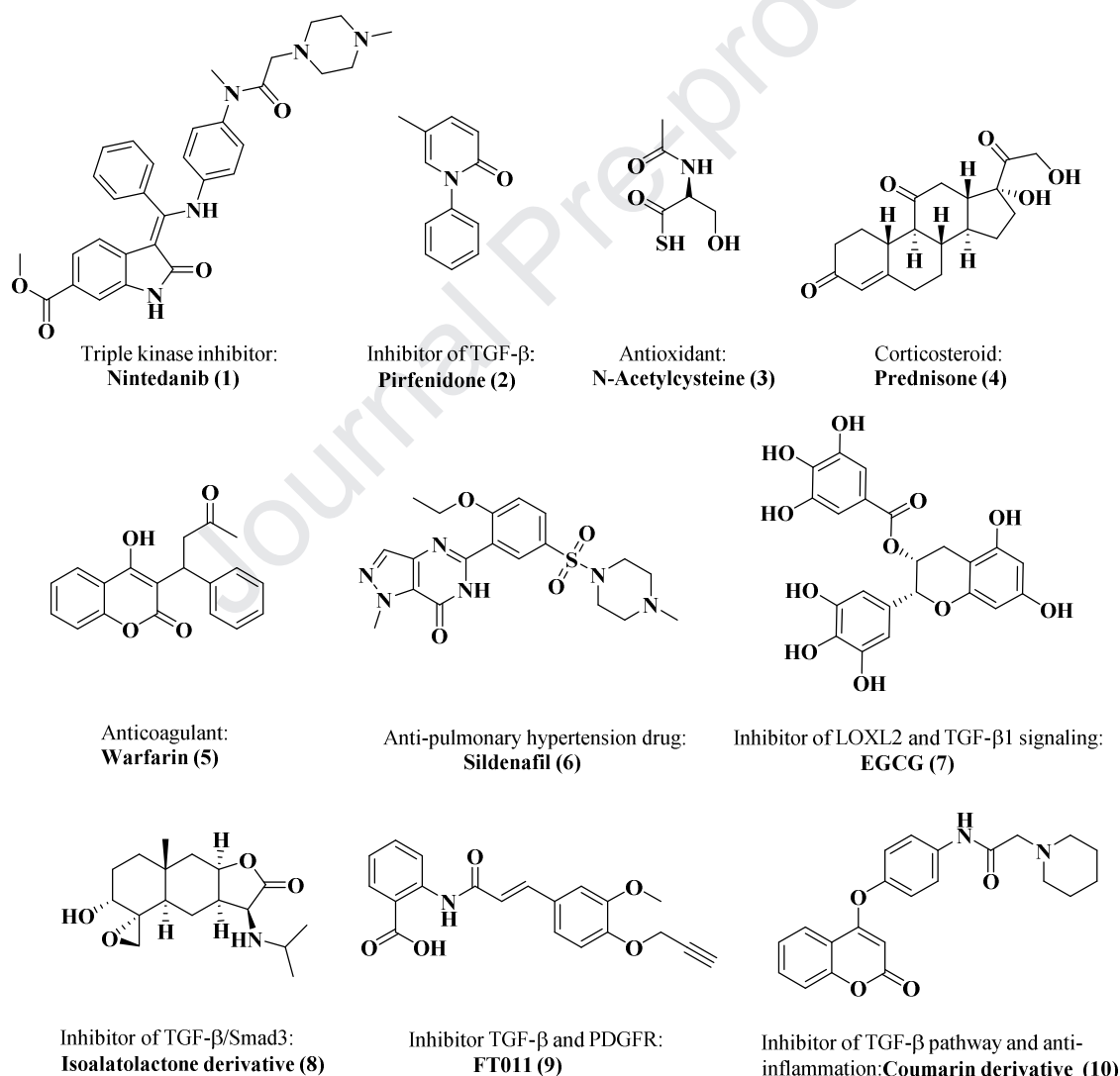
The treatment of pulmonary fibrosis progresses really slowly due to the unclear etiology and problems in accurate diagnosis. Except lung tissue transplantation, considering the characteristics and possible pathogenesis of IPF, drugs with various mechanisms had also been applied to the clinical treatment, such as antifibrotic agents (nintedanib, **1**, and pirfenidone **2**), antioxidants (N-Acetylcysteine, **3** [5]), corticosteroids (Prednisone, **4** [6]), immunomodulatory cytokines (Interferon gamma-1 β [7]), anticoagulants (Warfarin, **5** [8]), anti-gastroesophageal reflux agent (Proton pump inhibitors and antacid medication [9]), and anti-pulmonary hypertension drug (Sildenafil, **6** [10]) et al. (**Figure 1**). Up to now, only nintedanib (**1**) and pirfenidone (**2**) were approved by FDA for the treatment of IPF. The former was a multi-tyrosine kinase inhibitor mainly targeting VEGFR, FGFR and PDGFR, and

could consistently and significantly slow disease progression by reducing the annual rate of decline in forced vital capacity by approximately 50% versus placebo in IPF patients [11-13]. However, due to its poor oral bioavailability and metabolic instability [14], as well as side effects caused by off-target effects, nintedanib in clinical application also has limitations. Similar things happened to pirfenidone, an inhibitor for TGF- β production and TGF- β stimulated collagen production. Although clinical trials have demonstrated that it could reduce the decline in lung function in IPF patients, there are concerns about the adverse drug reactions. Post-marketing surveillance in Japan revealed that 24.3% of patients discontinued pirfenidone therapy because of adverse drug reactions [15]. Hence, efficient and also safety drugs were urgently needed for IPF treatment.

In recent years, the study of multiple cytokines in the lung has made important progress in the study of the mechanism of pulmonary fibrosis. Among the cytokines involved in pulmonary fibrosis, transforming growth factor TGF- β is the most deeply studied and plays an important role in the onset and progression of the disease [16]. TGF- β 1 plays an important role in regulation of inflammatory processes, ECM production, and stem cell differentiation as well as T-cell regulation and differentiation. Therefore, it is considered to be directly related to fibrosis. Inhibition of the binding of TGF- β to its receptor and the function of related Smad proteins become a critical strategy for anti-fibrosis recently. Except pirfenidone, the safety and scientific validity of Epigallocatechin-3-gallate (EGCG, **7**), a fibroblast specific inhibitor of LOXL2 and TGF- β 1 signaling, has now been evaluated in patients with

89 pulmonary fibrosis in the phase III clinical study in 2019 (NCT03928847).
 90 Isoalato lactone derivative **8** exhibited promising efficacy in a bleomycin-induced
 91 pulmonary fibrosis mice model through inhibition of TGF- β /Smad3 pathway [17].
 92 Cynamoyl anthranilate analogue FT011 (**9**) inhibited TGF- β 1 and PDGF-BB
 93 induced collagen production *in vitro*, and subsequent research showed that it also
 94 reduced the fibrotic scar in the diseased kidney [18].

95



96

97 **Figure 1.** Compounds reported for the treatment of idiopathic pulmonary fibrosis.

98

In our previous reports, compound **10**, a 4-substituted coumarins derivative, was found to be a promising, potential, orally active candidate for the treatment of fibrotic disease by its inhibition of TGF- β /Smad3 pathway and anti-inflammation efficacy [19]. However, the anticoagulant effect of coumarin scaffold may increase patient mortality during the treatment of pulmonary fibrosis, such as warfarin (5) [20]. Herein, considering that quinolone scaffold is widely used in the pharmaceutical field [21, 22], as well as the poor druggability of nintedanib due to its indolinone scaffold, bioisosteres and scaffold hopping [23] strategies were applied to design a new series of compounds bearing 2(1H)-quinolone scaffold (**Figure 2**). Hydrophobic heterocycles were also introduced to the terminal of 2(1H)-quinolone scaffold to explore its effects on biological activity. Finally, both *in vivo* and *in vitro* experiments were conducted to verify the anti-fibrotic effect and toxicity of these compounds, as well as the underlying mechanism.

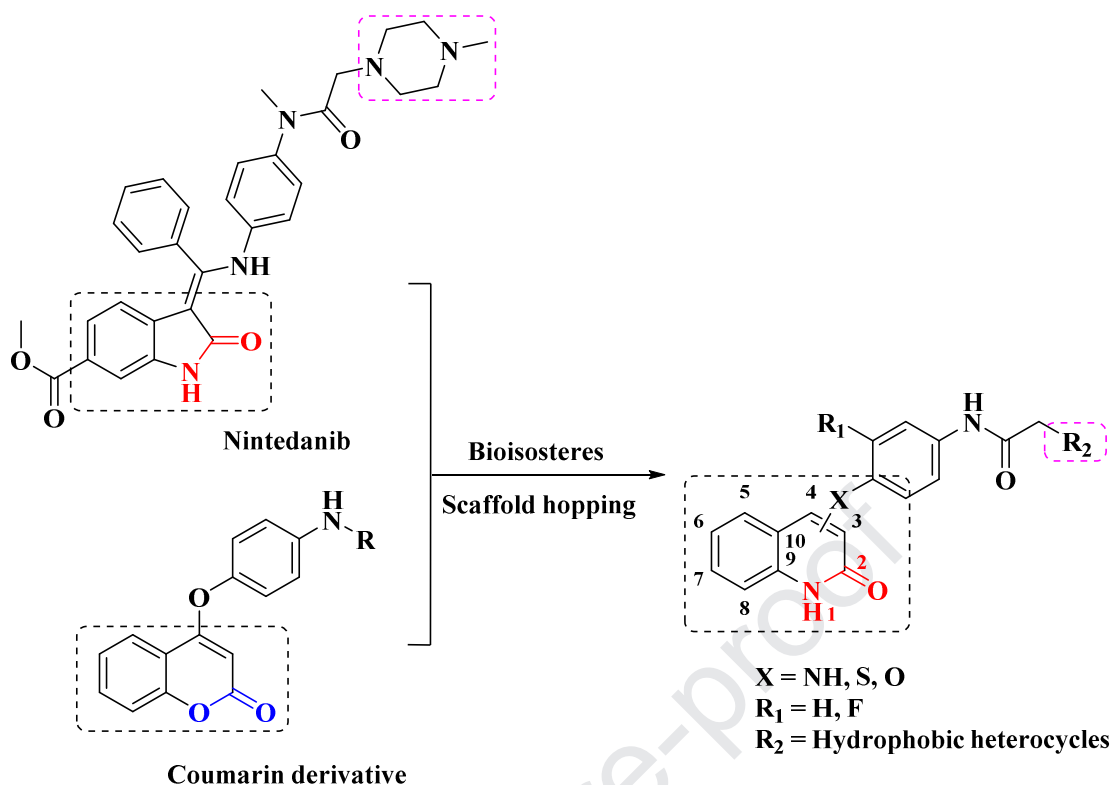


Figure 2. Design a novel series of compounds with anti-fibrotic effects by bioisosteres and scaffold hopping.

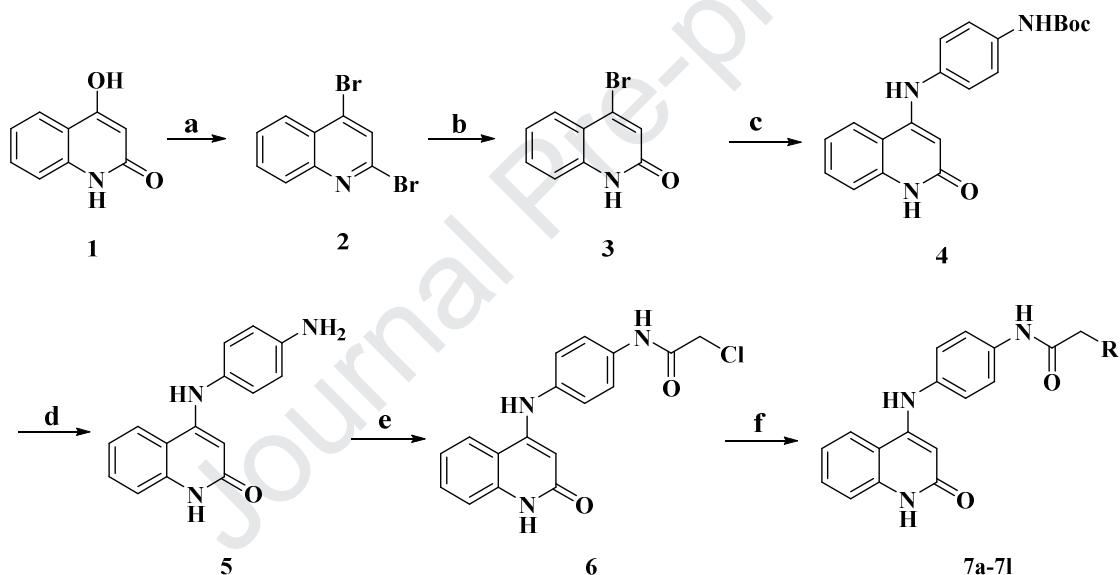
2. Chemistry

Considering the poor druggability of nintedanib and disadvantages of coumarin scaffold, we designed a series of compounds bearing 2(H)-quinolinone scaffold with different terminal substituent to improve its druggability. To be specific, we considered the influence of several factors on its *in vitro* activity: different hydrophobic groups at the terminal, different linker atoms between 2(H)-quinolinone and benzene ring, electron-withdrawing substituents in benzene ring, and different substitution locations in 2(H)-quinolinone.

4-Hydroxy-2(H)-quinolinone (**1**) was halogenated to obtain 2,

4-dibromoquinoline (**2**), and 4-bromoquinolin-2(1H)-one (**3**) was got by hydrolysis reaction. The important intermediate **4** comprised NH-linker was synthesized though Buchwald–Hartwig reaction catalyzed by Xantphos and $\text{Pd}_2(\text{dba})_3$. T-butyloxycarbonyl was removed under acidic conditions, and then the exposed amino group was reacted with chloroacetyl chloride to obtain important intermediate **6**. Specific methods were shown in **Scheme 1**.

Scheme 1. General procedure for the synthesis of compounds 7a-7l.

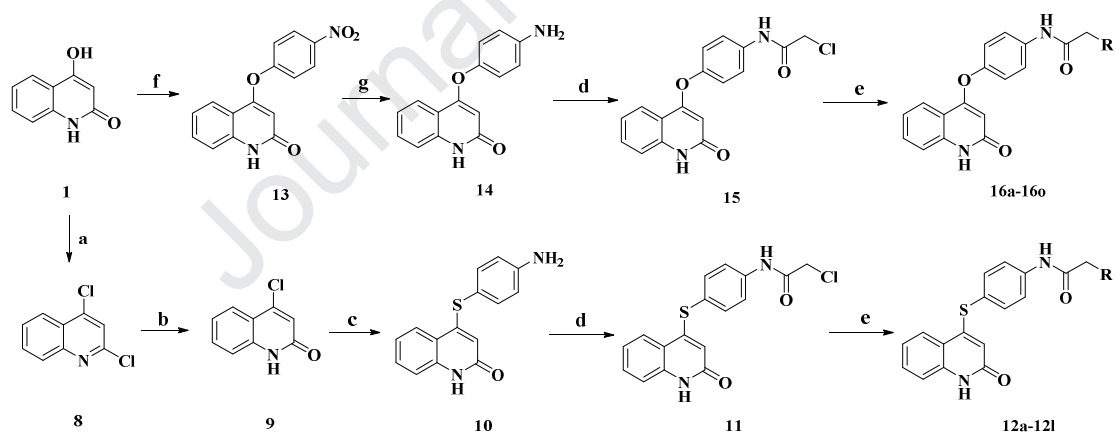


Reagents and conditions: (a) TBAB, P_2O_5 , toluene, 100°C , 6 h, 42%; (b) hydrobromic acid, 1,4-dioxane, 90°C , 4 h, 75%; (c) 4-(tert-butoxycarbonylamino)aniline, Xantphos, $\text{Pd}_2(\text{dba})_3$, t-BuOK, dioxane, 130°C , 24 h, 66%; (d) trifluoroacetic acid, rt, overnight, 92%; (e) chloroacetyl chloride, Et_3N , DMF, $0-25^\circ\text{C}$, 4 h, 95%; (f) RNH_2 , Et_3N , DMF, rt, overnight, 45-84%.

It was simpler to synthesize compound **12a-12l** when the linker atom was sulfur atom. 4-Hydroxy-2(H)-quinolinone (**1**) was reacted with POCl_3 and heated to 100°C to

get 2,4-dichloroquinoline (**8**), and 4-chloroquinolin-2(1H)-one (**9**) was obtained by hydrolysis reaction as the same method for 4-bromoquinolin-2(1H)-one (**3**). Lower reactivity intermediate **9** was stirred with K_2CO_3 and 4-aminobenzenethiol in DMF at $130^\circ C$ to obtain 4-((4-aminophenyl)thio)quinolin-2(1H)-one (**10**). Compound **16a-16o** with oxygen atom as the linker atom also started from 4-Hydroxy-2(H)-quinolinone (**1**), which was then stirred with 1-fluoro-4-nitrobenzene and K_2CO_3 in DMF at $100^\circ C$ to get 4-(4-nitrophenoxy) quinolin-2(1H)-one (**13**). Under the catalysis of iron powder and concentrated hydrochloric acid, nitro group was reduced to get intermediate **14** for subsequent reaction. Specific methods were shown in **Scheme 2**.

Scheme 2. General procedure for the synthesis of compounds 12a-12l and 16a-16o.



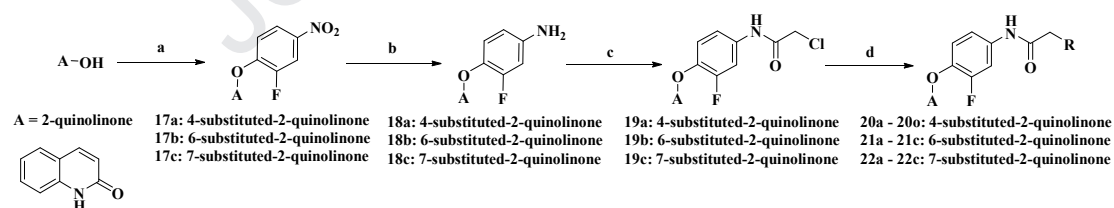
Reagents and conditions: (a) $POCl_3$, $100^\circ C$, 6 h, 65%; (b) hydrochloric acid, 1,4-dioxane, $90^\circ C$, 4 h, 73%; (c) 4-aminothiophenol, K_2CO_3 , DMF, $130^\circ C$, 6 h, 58%; (d) chloroacetyl chloride, Et_3N , DMF, $0^\circ C$, 4 h, 0-25%; (e) RNH_2 , Et_3N , DMF, rt, overnight, 62-90%; (f) 4-fluoronitrobenzene, K_2CO_3 , DMF, $100^\circ C$, 6 h, 72%; (g) Fe, HCl, MeOH / $H_2O = 9/1$, $85^\circ C$, 4 h, 90%.

The introduction of fluorine atom to the drug structure has been reported to

beneficially change its activities. A series of compounds containing fluorine atom on the benzene ring were synthesized to verify its biological activity *in vitro*. Due to the strong electrophilicity of 3,4-difluoronitrobenzene, it was stirred with 4-Hydroxy-2(H)-quinolinone (**1**) and K_2CO_3 in DMF at room temperature without heating to obtain 4-(2-fluoro-4-nitrophenoxy)quinolin-2(1H)-one (**17**). Subsequent route to synthesize compounds **20a-20o** (Scheme 3) was similar to that of compound **16a-16o**.

In order to explore the effect of the substituent position of the 2-hydroxyquinoline skeleton on its activity, we then tried to connect the substituents at the C-6 and C-7 positions and synthesized compounds **21a-21c** and **22a-22c**. Specific and subsequent routes to synthesize these compounds are shown in Supporting Information (Scheme S1).

Scheme 3. General procedure for the synthesis of compounds 20a-20o, 21a-12c, and 22a-22c.



Reagents and conditions: (a) 3,4-difluoronitrobenzene, K_2CO_3 , DMF, rt, overnight; (b) Fe, HCl, MeOH/H₂O = 9/1, 85°C, 4 h; (c) chloroacetyl chloride, Et₃N, DMF, 0°C, 4 h, 95%; (d) RNH₂, Et₃N, DMF, rt, overnight.

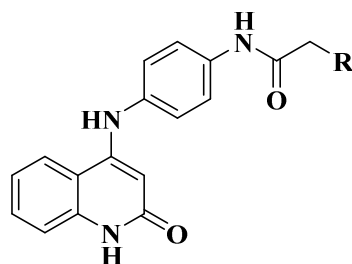
3. Results and discussion

3.1 Anti-fibrotic activity of compounds on NRK-49F cells *in vitro*.

Fibrosis is characterized by excessive collagen deposition between the cells of diseased tissues. Thus, the *in vitro* screening cell model was established to determine the deposited collagen amount between cells. According to our previous published and other reports [19, 24, 25], TGF- β -induced NRK-49F cells (rat fibroblast cells) produce a large amount of intercellular collagen deposition that is similar to the characteristic of fibrosis. Thus, we adopted it as an effective and convenient *in vitro* screening model for anti-fibrotic evaluation. The inhibition rates of collagen deposition for all synthesized compounds were subsequently tested on TGF- β -induced NRK-49F cells at a concentration of 10 μ M. Simultaneously, the survival rates (SR) of NRK-49F cells were also tested by MTT assay to verify their *in vitro* toxicities.

Compounds **7a-7l** with different terminal substituent were synthesized initially under the inspiring of nintedanib, which own same nitrogen atom as linker atom. As shown in **Table 1**, most of compounds had weaker collagen deposition inhibition effects in compared with nintedanib. However, we found that nintedanib exhibited significantly toxicity to NRK-49F cells judging from low survival rate of NRK-49F cells (40% survival rate (SR)). Interestingly, **7i** showed relatively strong collagen deposition inhibition effect and low toxicity to NRK-49F cells among them (73% inhibition rate (IR)). Whether the Boc group with a large steric hindrance at the terminal of its structure resulted in its activity improvement still needed further confirmation.

Table 1. Collagen accumulation IR and cell SR of 7a-7l.



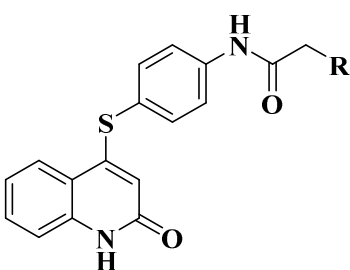
7a-7l

Cpd	R	IR (%)	SR (%)	Cpd	R	IR (%)	SR (%)
7a		59.91 ± 7.61	72.49 ± 3.82	7g		38.97 ± 0.31	72.55 ± 3.47
7b		24.42 ± 2.68	75.40 ± 1.12	7h		50.20 ± 2.12	83.49 ± 1.65
7c		40.86 ± 2.99	81.91 ± 3.66	7i		73.34 ± 2.85	67.52 ± 4.96
7d		20.08 ± 6.43	82.55 ± 0.33	7j		49.99 ± 1.47	83.55 ± 6.48
7e		38.93 ± 1.31	78.04 ± 3.33	7k		44.24 ± 6.94	82.58 ± 2.22
7f		45.95 ± 5.34	64.78 ± 2.66	7l		28.71 ± 5.19	83.71 ± 0.94
nintedanib						95.47 ± 2.65	40.02 ± 2.46

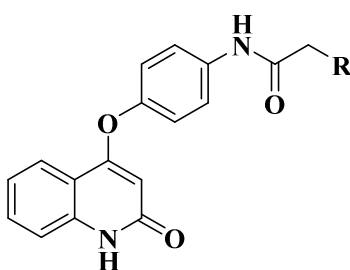
Inhibitory effects against TGF- β -induced total collagen accumulation in NRK-49F cells at a concentration of 10 μ M. Cell survival rate is calculated by MTT assay. The results are the means \pm SD of at least three independent experiments.

Bioisosteric replacement and scaffold hopping are two techniques widely applied in structural optimization of lead compounds to reduce toxicity and improve activity. To be specific, when the linker atoms nitrogen atom in compounds **7a-7l** was substituted by sulfur atom or oxygen atom, the effects of linker atoms on biological activity were evaluated and discussed. The results were listed in **Table 2**.

216 **Table 2. Collagen accumulation IR and cell SR of 12a-12l and 16a-16o.**



12a-12l



16a-16o

12a-12l				16a-16o			
Cpd	R	IR (%)	SR (%)	Cpd	R	IR (%)	SR (%)
12a		80.88 ± 2.39	87.05 ± 5.13	16a		68.05 ± 6.38	82.21 ± 2.74
12b		28.37 ± 7.65	93.46 ± 2.63	16b		27.42 ± 5.41	78.46 ± 1.95
12c		53.38 ± 4.78	77.44 ± 3.37	16c		59.27 ± 3.89	95.74 ± 4.54
12d		28.59 ± 8.17	115.78 ± 4.55	16d		31.52 ± 7.86	79.92 ± 6.73
12e		39.97 ± 7.03	86.69 ± 3.93	16e		43.66 ± 4.42	80.18 ± 1.33
12f		56.57 ± 0.88	77.95 ± 1.93	16f		78.33 ± 3.57	92.17 ± 2.11
12g		39.38 ± 3.02	101.31 ± 4.3	16g		50.02 ± 11.41	96.28 ± 5.24
12h		51.14 ± 2.05	80.31 ± 4.37	16h		43.92 ± 4.78	81.22 ± 2.61
12i		72.37 ± 6.87	71.25 ± 4.26	16i		76.24 ± 4.15	75.60 ± 4.72
12j		52.97 ± 2.21	83.92 ± 3.41	16j		73.23 ± 5.47	92.67 ± 2.31
12k		58.62 ± 9.83	85.49 ± 5.88	16k		86.07 ± 2.02	96.26 ± 2.44
12l		51.09 ± 7.84	87.69 ± 8.85	16l		25.36 ± 3.25	89.24 ± 2.64
16m		58.11 ± 2.23	95.14 ± 1.09	16o		41.73 ± 8.79	91.69 ± 3.34
16n		46.02 ± 5.45	96.04 ± 3.82	nintedanib		95.47 ± 2.65	40.02 ± 2.46

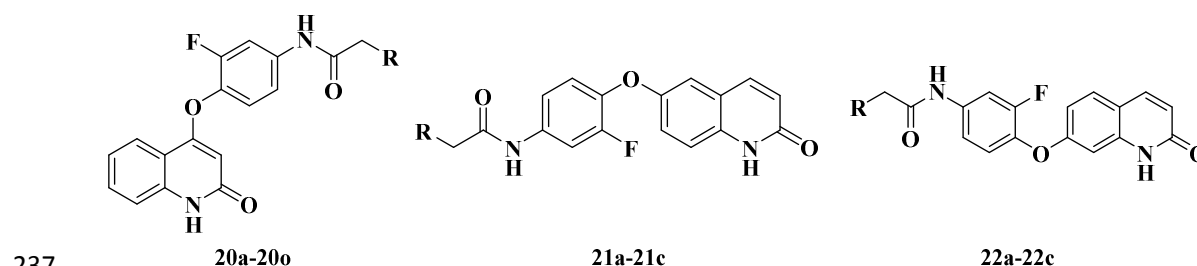
Inhibitory effects against TGF- β -induced total collagen accumulation in NRK-49F cells at a concentration of 10 μ M. Cell survival rate is calculated by MTT assay. The results are the means \pm SD of at least three independent experiments.

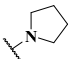
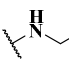
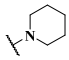
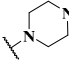
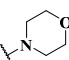
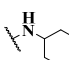
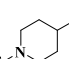
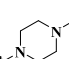
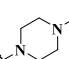
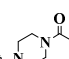
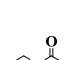
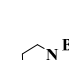
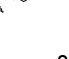

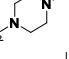
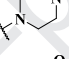
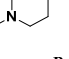
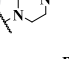
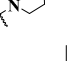
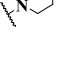
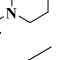
221

As shown in **Table 2**, compared with **7a-7l**, the collagen inhibition rate and cell survival rate among **12a-12l** and **16m-16o** have been improved to some extent when the NH-linker was replaced by S-linker or O-linker, respectively. Among them, compound **12a** in S-linker series and **16k** in O-linker series showed good collagen inhibition rate (80% and 86%) and low toxicity (13% and 4%). Compounds **7i**, **12i** and **16i** with the terminal Boc group demonstrated relatively acceptable *in vitro* anti-fibrotic activities (73%, 72% and 76%). However, when the terminal Boc group was removed (**16m**), it exhibited poor *in vitro* activity (58%), suggesting that a hydrophobic group with a large spatial position at the terminal might be beneficial for anti-fibrotic activity *in vitro*. In order to verify our suspicions, compound **16f** and **16j** with similar steric hindrance groups and less susceptible to metabolism were subsequently synthesized. Results showed that hydrophobic group with a large spatial position at the terminal did play crucial parts in collagen accumulation inhibition.

235

236 **Table 3. Collagen IR and cell SR of 20a-22o, 21a-21c, and 22a-22c.**



Cpd	R	IR (%)	SR (%)	Cpd	R	IR (%)	SR (%)
20a		49.49 ± 6.52	96.43 ± 2.47	20l		50.57 ± 5.93	99.35 ± 1.12
20b		38.27 ± 4.76	87.18 ± 3.07	20m		60.27 ± 2.16	93.31 ± 2.29
20c		47.28 ± 7.12	90.77 ± 1.71	20n		53.92 ± 7.32	90.8 ± 1.44
20d		45.94 ± 2.55	104.93 ± 3.04	20o		49.07 ± 4.19	89.61 ± 7.28
20e		73.87 ± 5.12	98.95 ± 0.82	21a		34.57±3.54	95.19 ± 3.13
20f		87.53 ± 3.05	97.52 ± 2.26	21b		57.43±3.59	85.62 ± 2.31
20g		42.73 ± 6.36	108.38 ± 3.04	21c		61.53±3.21	83.32 ± 4.24
20h		60.74 ± 6.01	98.59 ± 3.56	22a		56.59±2.67	98.23 ± 3.25
20i		89.13 ± 3.97	86.18 ± 5.65	22b		76.37±2.78	89.65 ± 2.36
20j		78.04 ± 3.94	93.11 ± 4.78	22c		67.72±5.45	89.77 ± 3.41
20k		58.81 ± 6.03	106.12 ± 2.32	nintedanib		95.47 ± 2.65	40.02 ± 2.46

238 Inhibitory effects against TGF- β -induced total collagen accumulation in NRK-49F cells at a
 239 concentration of 10 μ M. Cell survival rate is calculated by MTT assay. The results are the means \pm
 240 SD of at least three independent experiments.

241

242 Next, compounds with fluorine atom substitution on benzene ring were designed
 243 for both biological activity bioavailability improvements. As shown in **Table 3**, most
 244 compounds with fluorine substitution demonstrated better anti-fibrotic effects and
 245 lower cytotoxicity than their corresponding compounds **16a-16o**. **20m** possessed
 246 weaker anti-fibrotic activity and less cytotoxicity than compound **20i** owning Boc

group (similar to compounds **16i** and **16m**).

Finally, **21a-21c** and **22a-22c** were synthesized to investigate the anti-fibrosis effect of substitution at different positions on the 2(1H)-quinolone. **21a-21c** owning substitution at C-6 position showed significant decrease in anti-fibrotic activity *in vitro*, which is similar to compounds **22a-22c** substituted at C-7 position. Compounds **20f**, **20i** and **20j** with excellent bioactivity *in vitro* and low toxicities were further selected as candidate compounds for further *in vitro* experiments.

In general, the initial structure-activity relationship could be concluded as follows: firstly, the linker atom affects the cytotoxicity of these compounds. Compounds with oxygen atom as the linker demonstrated the lowest cytotoxicity than those with nitrogen atom and sulfur atom. Secondly, hydrophobic groups with larger steric hindrance at the end of the piperazine ring contributed greatly to the anti-fibrotic activities but caused greater cytotoxicities such as **7i**, **12i**, and **16i**. Then, the introduction of fluorine atom on the benzene ring was beneficial to enhance anti-fibrotic activity and reduce cytotoxicity to some extent. Finally, substitution at C-6 and C-7 position decreased anti-fibrotic activity and showed a little cytotoxicity effect to NRK-49F cells. However, compounds **12a** with tetrahydropyrrole and **16k** with diethylamine due to some certain exceptions also exhibited excellent anti-fibrotic activity *in vitro*, which was inconsistent with the basic structure-activity relationship. Taken together, five compounds of **12a**, **16k**, **20f**, **20i**, and **20j** with potential anti-fibrosis activities were selected for further determination of IC₅₀ values with potential anti-fibrosis activities. As exhibited in **Table 4**, those five compounds

showed an order of magnitude of inhibitory activity with nintedanib against TGF- β -induced total collagen accumulation in NRK-49F cells with IC₅₀ range between 3.89 and 6.12 μ M.

Table 4. IC₅₀ values against TGF- β -induced total collagen accumulation in NRK-49F cells.

Entry	IC ₅₀ (μ M)	Entry	IC ₅₀ (μ M)
12a	5.33 \pm 0.35	16k	5.27 \pm 0.42
20f	3.89 \pm 0.46	20i	6.12 \pm 0.32
20j	4.47 \pm 0.52	nintedanib	1.10 \pm 0.13

The results are the means \pm SD of at least three independent experiments.

Collagen fibers between cells were straightforward visualized through Sirius Red staining. It was found that **12a**, **16k**, **20i**, **20j** and **20f** could significantly reduce the production of filamentous collagen (**Figure 3**). Moreover, it's also worth noting that the cell number of TGF- β -induced NRK-49F cells left after treatment of these compounds was much higher than that of nintedanib, which was consistent with MTT results, indicating that **12a**, **16k**, **20i**, **20j** and **20f** were safer than nintedanib.

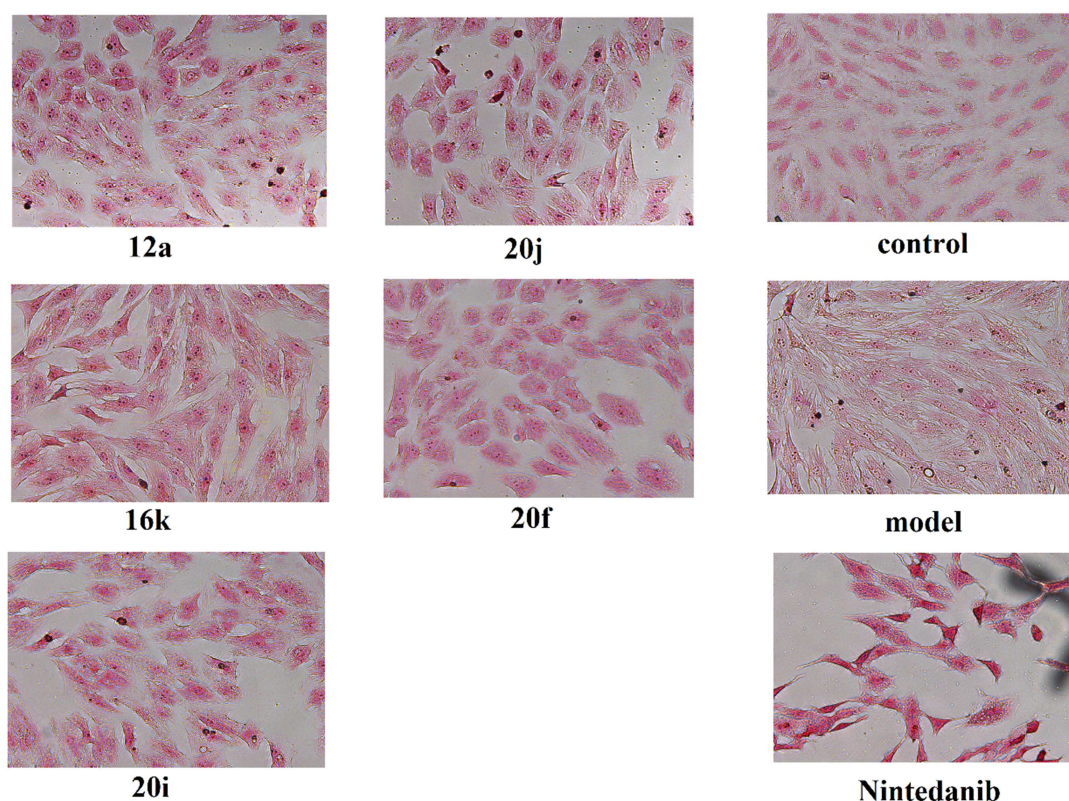


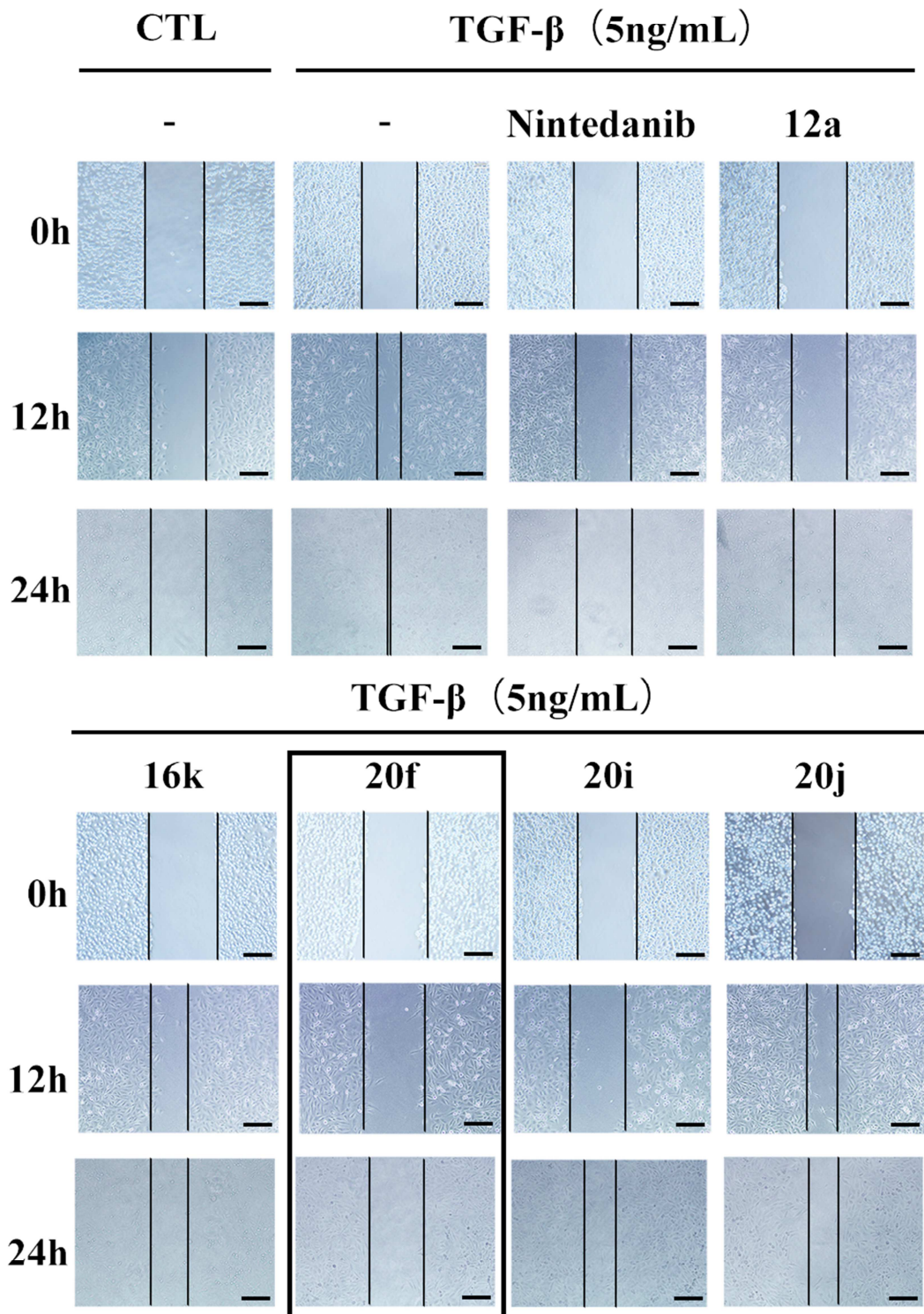
Figure 3. Picro-Sirius Red (PSR) staining for the total collagen accumulation induced by TGF- β in NRK-49F cells.

3.2 12a, 16k, 20f, 20i and 20j inhibited TGF- β -induced fibroblasts migration

Fibroblasts migration to the fibrotic lesions stimulated by concomitant cytokines (like TGF- β 1) plays an important role in pulmonary fibrosis [26], so inhibiting fibroblasts migration can delay the process of pulmonary fibrosis.

Accordingly, the effects of selected compounds on cell migration was accessed by wound healing assays. The results indicated that **12a**, **16k**, **20f**, **20i**, **20j** and nintedanib could inhibit TGF- β -induced migration of mouse fibroblast L929 cells at different level with a concentration of 10 μ M, while **20f** exhibited the best anti-migration capacity (**Figure 4**). Hence, **20f** was finally chosen as further

296 antifibrotic evaluation and mechanism investigation both *in vitro* and *in vivo*.



297

298 **Figure 4.** Wound healing assay were performed to access the inhibition effects of fibroblast

299 migration by **12a**, **16k**, **20f**, **20i**, **20j** and nintedanib. L929 cells were treated with/without TGF- β

(5 ng/mL) and compounds (10 μ M). Data were collected after 12 and 24 hours.

3.3 20f inhibited protein expression of collagen I and α -SMA in TGF- β -induced NRK-49F Cells.

α -Smooth muscle actin (α -SMA) in myofibroblasts [27] and excessive collagen I deposition [28] in extracellular matrix were hallmarks of fibrosis. Therefore, the abilities of **20f** to suppress protein expression of α -SMA and collagen I were investigated *in vitro*. As shown in **Figure 5**, the protein expression levels of α -SMA and collagen I were obviously over-expressed in TGF- β -induced NRK-49F cells, whereas treatment with **20f** or nintedanib significantly inhibited their expressions, suggesting that both **20f** and nintedanib inhibited α -SMA expression and collagen accumulation in the response to TGF- β stimulation.

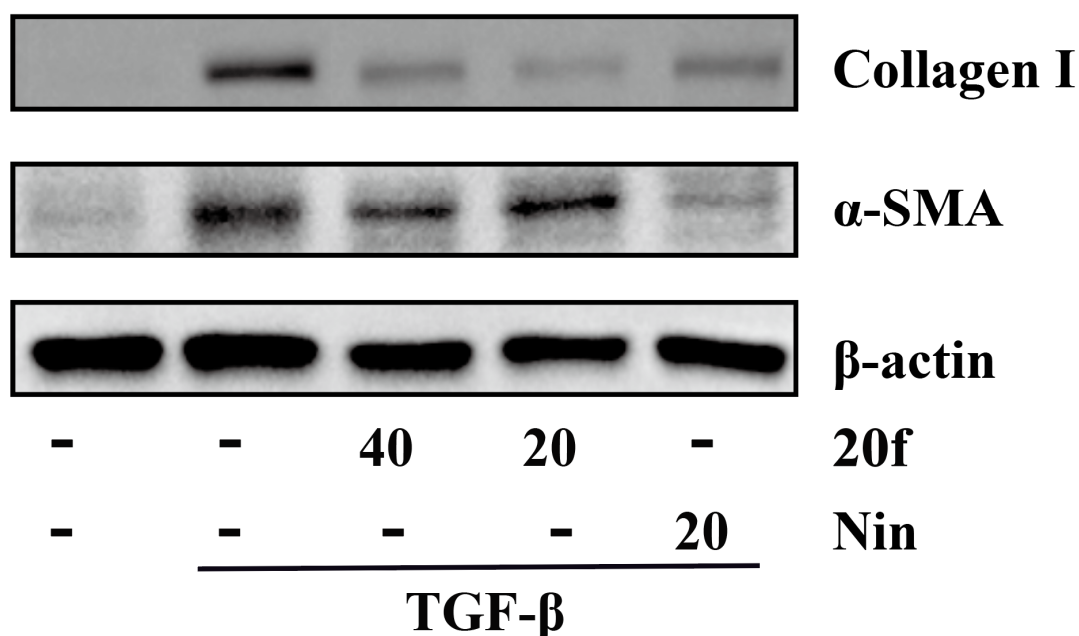


Figure 5. Protein expression levels of Collagen I and α -SMA were probed through western blot.

NRK-49F cells were treated with/without TGF- β (5 ng/mL) and compound **20f** (20 and 40 μ M)

for 24 h. β -actin was used as a loading control.

3.4 20f exhibited anti-fibrotic activity by inhibiting TGF- β /Smad2/3-dependent and independent pathways.

Since activation of Smad pathway is the primary downstream signaling pathway of TGF- β and Smad proteins have been implicated in bleomycin-induced lung fibrosis [29], the expression of total and phosphorylated Smad2 and Smad3 were further detected by immunoblot to test the hypothesis that **20f** might block the primary step of TGF- β signaling via the regulation of Smads.

As shown in **Figure 6A**, TGF- β stimulation significantly increased the phosphorylation levels of Smad2 and Smad3, whereas treatment with **20f** significantly reduced this phosphorylation in a dose dependent manner. However total Smad2 and Smad3 proteins were constitutively expressed and were not affected by TGF- β or **20f** treatment.

Smad3-independent pathway including the ERK1/2 [30] and p38 MAP kinase [31] has also been reported in TGF- β -induced fibrosis [32]. Activated ERK1/2 and p38 in turn conveys the signal to the Smad2/3 via phosphorylation and active the Smad signaling pathway. Therefore, the TGF- β /Smad2/3-independent pathway was further explored. NRK-49F cells were cultured with or without TGF- β in the presence or absence of **20f** for indicated times. As shown in **Figure 6B**, TGF- β stimulation obviously increased the phosphorylation level of ERK1/2 and p38, whereas cotreatment with **20f** significantly inhibited their phosphorylation levels of ERK1/2 and p38. Both total p38 and ERK1/2 were constitutively expressed and were not

affected by TGF- β or **20f** treatment.

On the basis of these observations, it could be concluded that **20f** ameliorated fibrosis by inhibiting both TGF/Smad2/3-dependent and independent pathways, including Smad2, Smad3, ERK and p38 phosphorylation.

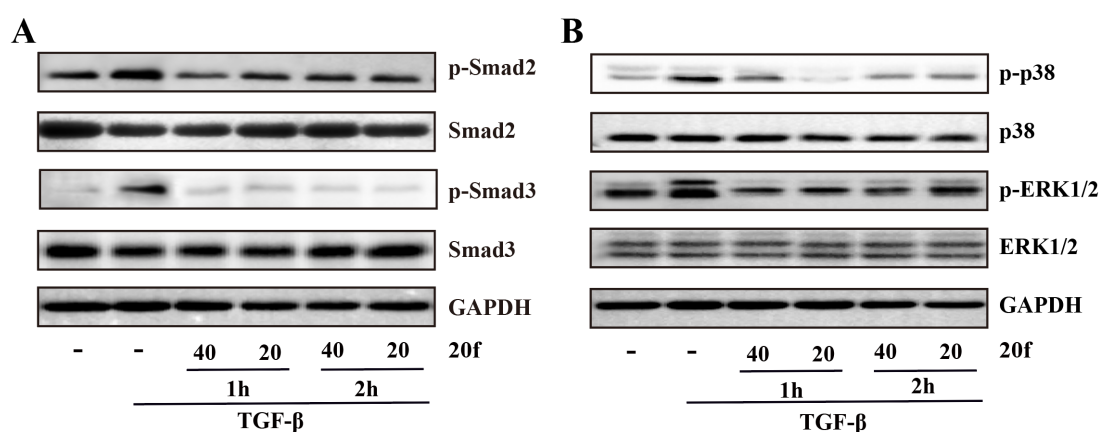


Figure 6. (A) Effects of **20f** on TGF- β -induced phosphorylation of Smad2 and Smad3 in NRK-49F cells. NRK-49F cells were treated with/without **20f** (20 and 40 μ M) for 1 and 2 hours and then treated with TGF- β (5 ng/mL) for 1h. (B) Effects of **20f** on TGF- β -induced phosphorylation protein expression of p38 and ERK1/2 in NRK-49F cells. NRK-49F cells were treated with/without **20f** (20 and 40 μ M) for 1 and 2 hours and then treated with TGF- β (5 ng/mL) for 1h. GAPDH was used as a loading control.

3.5 Pharmacokinetic experiment of **20f**.

The plasma concentration–time curves for **20f** after a single dose in rats were shown in **Figure S1 (Supporting Information)**. The plasma concentrations of **20f** rapidly reached peak, and gradually declined after oral administration. As shown in **Table 5**, the oral bioavailability of **20f** was determined to be 41.55% (n = 5), much

better than nintedanib (approximately 12% in rats [20]).

Table 5. Pharmacokinetic parameters for 20f in SD rats.

Compound	20f	
	Intravenous injection	Oral administration
dose (mg/kg)	5	5
t _{max} (h)	0.08	4.33
t _{1/2} (h)	4.39	3.5
AUC _{0-t} (μg/L*h)	13149.76	5463.86
F (%)		41.55

3.6 Effects of 20f on Bleomycin-induced pulmonary fibrosis model.

To further verify anti-fibrotic potency of **20f** *in vivo*, two bleomycin induced lung fibrosis models (one for prevention model and the other one for treatment model) were employed in our study. Mice challenged with BLM (3 U/kg) at day 0 were treated with **20f** (50 or 100 mg/kg) and nintedanib (50 mg/kg) at day 1 for prevention model and the whole administration process last for 30 days. For treatment model, every experimental setting was the same except that both compounds were administrated only from day 8 to day 21 (**Figure 7A**). Survival rates, hydroxyproline (an indicator of collagen deposition) level, histologic analysis (Masson's trichrome staining, hematoxylin and eosin (H&E) staining and immunocytochemistry) were further performed to evaluate anti-fibrosis effects of **20f**.

As shown in **Figure 7B**, in prevention model, **20f** (50 or 100 mg/kg) demonstrated comparable survival rate with nintedanib (50 mg/kg). However, in treatment model, **20f** (50 mg/kg) showed better survival rate than nintedanib. BLM

induction resulted in a large amount of collagen to deposit in lung tissue in model group, which was consistent with the hydroxyproline result (**Figure 7C and 7D**). Both **20f** and nintedanib could inhibit collagen deposition and reduce hydroxyproline content in lung tissue in prevention model. However, when treatment started at day 8 (treatment model), there was no significant difference in the reduction of collagen deposition in nintedanib group in comparison with model group. In contrast, **20f** still showed a significant blocking effect on collagen accumulation, particularly at high doses (100 mg/kg) (**Figure 7D**).

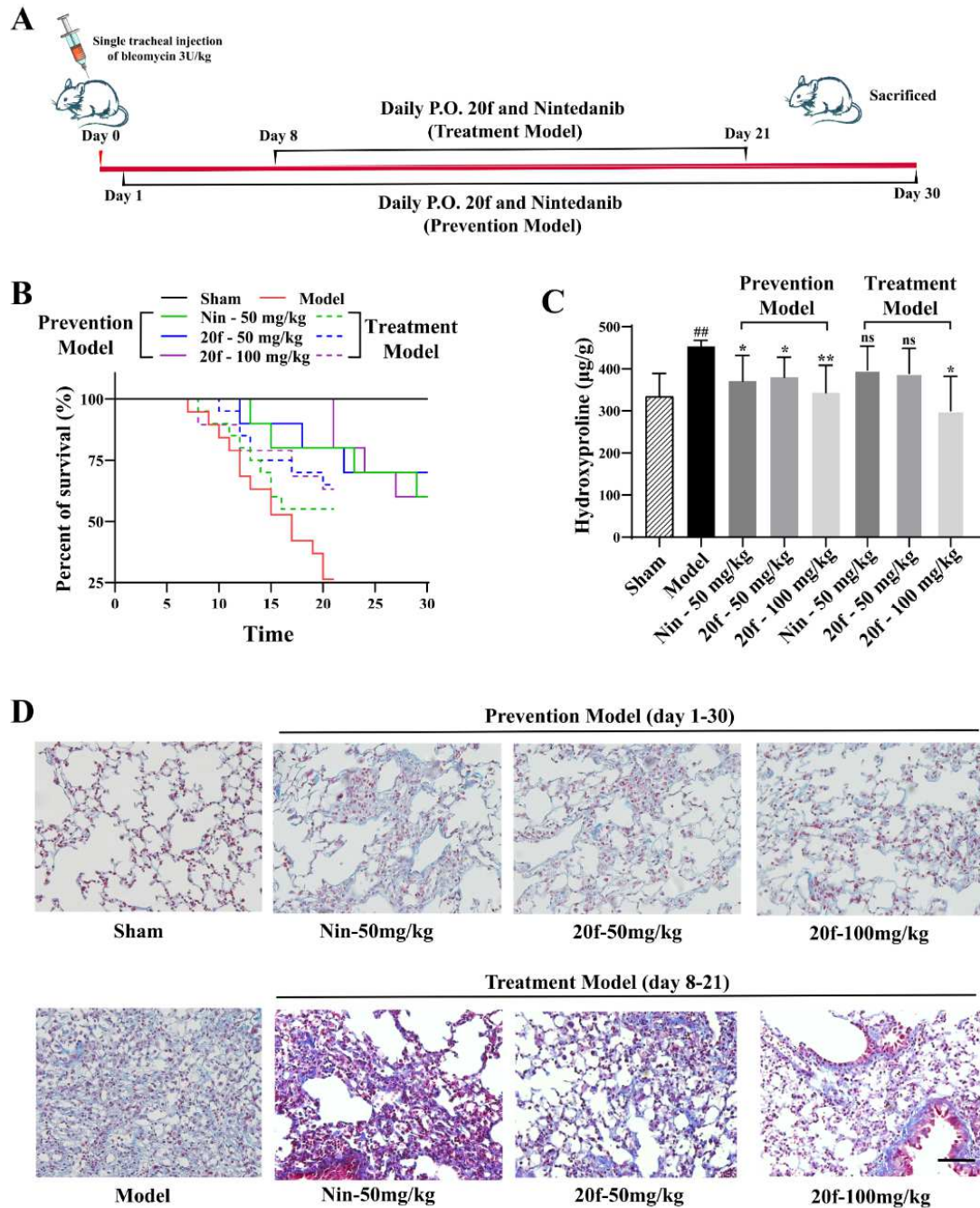


Figure 7. The anti-fibrotic potencies of 20f *in vivo*. C57BL/6 male mice were intratracheal instilled with BLM (3 U/kg) to induce pulmonary fibrosis, and the lungs were harvested at the end of experiment for the following analyses. (A) Dosing schedule of prevention model (day 1-30) and treatment model (day 8-21). (B) Survival curves of 20f and nintedanib for pulmonary fibrosis. (C) Hydroxyproline contents in lung tissues of each group were measured as described in the methods section. (D) Representative images demonstrating masson's trichrome of lung tissues

from experimental groups as indicated in Experiment section. Scale bars, 100 μ m. Data were presented as means (SD of the group. * $p < 0.05$, ** $p < 0.01$, compared with the BLM treatment. BLM, bleomycin; Nin, nintedanib.)

Both the Ashcroft scores and H&E staining were also used to evaluate the anti-fibrosis effects of **20f**. Results demonstrated that the lung tissues were fiercely damaged in mice instilled with BLM (**Figure 8A** and **8B**), whereas administration with **20f** and nintedanib notably protected the alveolar tissue structure (red arrow) and ameliorated the infiltration of inflammatory cells (yellow arrow) in prevention model (**Figure 8A**, upper panel). However, in the treatment model, delayed treatment with nintedanib at day 8 failed to ameliorate fibrosis, **20f** (100 mg/kg) still exhibited the ability to protect structure of lungs (**Figure 8A**, lower panel). These findings implicated that **20f** showed potentially promising therapeutic effects in both prevention and treatment models of pulmonary fibrosis.

To further validate the mechanism of **20f** *in vivo*, the phosphorylation level of Smad3 in lungs tissues was tested. As depicted in **Figure 8C**, BLM-induced mice elevated level of Smad3 phosphorylation in lung tissues. Relative to nintedanib, oral administration of **20f** could more effectively suppress Smad3 phosphorylation level, which was in accordance with the immunoblot results in **Figure 6**.

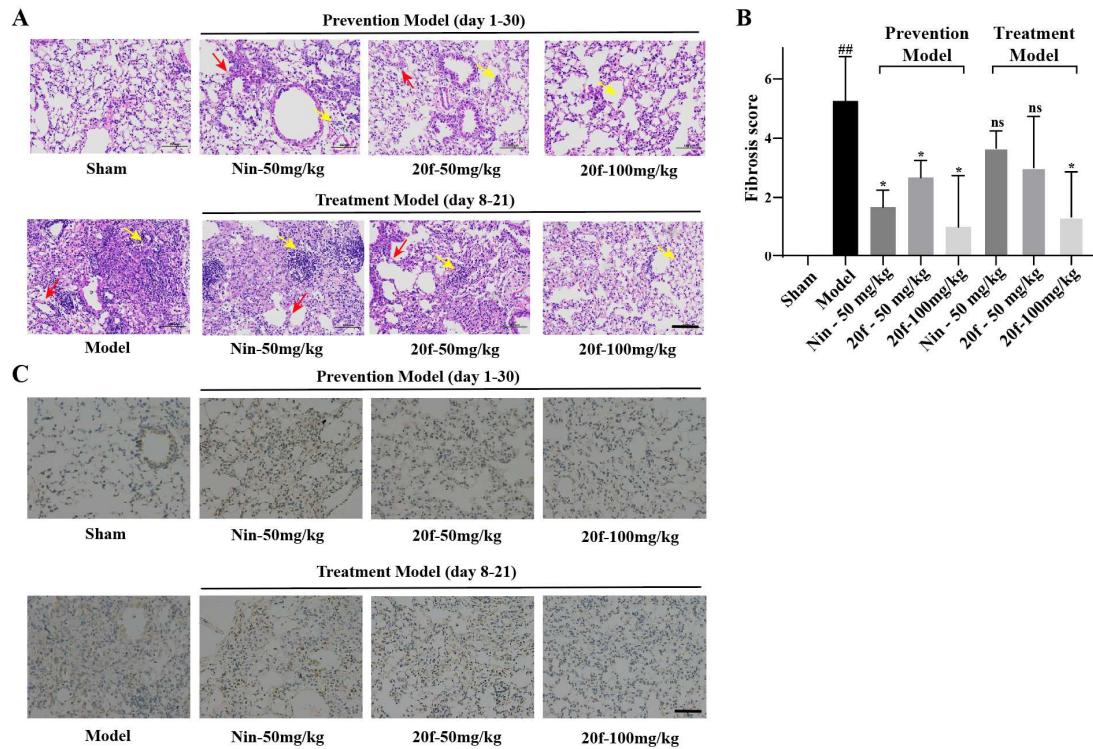


Figure 8. (A) Representative images demonstrating hematoxylin and eosin (H&E) staining of lung tissues from experimental groups as indicated in experiment section. (B) Ashcroft scores of lung tissues from experimental groups as indicated in experiment section. (C) Representative images demonstrating p-Smad3 staining of lung tissues from experimental groups as indicated in experiment section. Scale bars, 100 μ m. Data were presented as means (SD of the group. * $p < 0.05$, ** $p < 0.01$, compared with the BLM treatment. BLM, bleomycin. Nin, nintedanib.)

Taken together, **20f** exhibited beneficial therapeutic effects, specifically in survival rate improvement, collagen deposition decrease in lung tissue, as well as the lung tissue protection. Further immunohistochemical experiments showed that **20f** also inhibited phosphorylated expression level of Smad3, which was downstream of TGF- β pathway, and eventually contributed to its anti-fibrosis effect.

4. Conclusion

In this study, a series of compounds bearing 2(1H)-quinolone scaffold inspired by bioisosteres and scaffold hopping strategies were designed and synthesized, and then their anti-fibrotic effects were evaluated *in vitro*. **20f** was further selected to perform the mechanism studies due to its excellent collagen deposition inhibition in NRK-49F cells, low cytotoxicity, as well as decent anti-migration activity in L929 cells. Mechanism studies showed that **20f** significantly suppress the expression of fibrogenic phenotypic protein (such as α -SMA and collagen \square) *in vitro* by western blot analysis. Additionally, it also decreased the phosphorylation level of Smad 2/3, ERK and p38, indicating that TGF- β /Smad signaling pathway played crucial roles for collagen deposition reduction. Moreover, **20f** (50 and 100 mg/kg/day, p.o.) effectively alleviated collagen deposition in lung tissue and delayed the destruction of lung tissue structure in both prevention and treatment models. It was worth noting that **20f** demonstrated better survival rate than nintedanib. Subsequent immunohistochemical experiments further showed that the expression level of phosphorylated Smad3 in the lung tissue cells significantly declined after treatment with **20f**. All these phenomena and results illustrated **20f** effectively alleviated lung damage induced by intratracheal instillation of bleomycin in mice, and these beneficial effects should attribute to its inhibition of TGF- β /Smad dependent and in-dependent pathway as well as its low cytotoxicity. Considering the excellent bioavailability (F = 41.55%) and suitable eliminated half-life time ($T_{1/2}$ = 3.5 h), **20f** could be a potential drug candidate for the treatment of IPF.

5. Experimental

5.1 Chemistry.

All the chemical solvents and reagents used in this study were analytically pure without further purification and commercially available. TLC was performed on 0.20 mm silica gel 60 F₂₅₄ plates (Qingdao Ocean Chemical Factory, Shandong, China). Visualization of spots on TLC plates was done by UV light and I₂. NMR data were measured for ¹H NMR at 400 MHz and for ¹³C NMR at 101 MHz on a Bruker Avance 400 spectrometer (Bruker Company, Germany) using TMS as an internal standard. Mass spectra (MS) were obtained by a Q-TOF Premier mass spectrometer (Micromass, Manchester, UK). Purification of the final compounds were performed with reverse phase high-performance liquid chromatography (RP-HPLC). All final compounds were purified to ≥95% chemical purity as determined by HPLC with UV detection at 254 nm. Further details on the analytical conditions used for individual compounds may be found in the Supporting Information.

General procedure for synthesis of Phenylenediamine derivative.

2,4-dibromoquinoline (2). 4-hydroxyquinolin-2(1H)-one (4.83 g, 0.03 mol) and TBAB (19.32 g, 0.06 mol) were dissolved in methylbenzene (400 ml) in an oven-dried round bottom flask. Then P₂O₅ (17.04 g, 0.12 mol) was added dropwise to the reaction mixture in 1 hour. At the same time, the reaction mixture was heated to 100 °C and stirred at 100 °C for another 6 h. After the reaction was finished monitored by TLC, the solution was cooled to room temperature and alkalify to pH 9 with ice NaHCO₃

saturated solution. The organic phase was separated and dried over anhydrous Na_2SO_4 , then evaporated under vacuum to obtain an oil-like black product. Petroleum ether (200 ml) was added to the crude product and stirred about 30 minutes. The mixture was filtered, then the filter liquor was collected and dried in vacuum to obtain compound 2 as a yellow solid (3.61 g, 42% yield) without further purification. MS (ESI^+): $[\text{M} + \text{H}]^+$ calculated for $\text{C}_9\text{H}_5\text{NBr}_2$, 284.8789; found, 285.8901.

4-bromoquinolin-2(1H)-one (3). Compound 2 (3.5 g, 0.012 mol) was dissolved in 1,4-dioxane (30 ml) in a round bottom flask and heated. Hydrobromic acid which consisted of 60% water (30 ml) then was added to the mixture after it was heated to 90°C . The reaction mixture was stirred at 90°C after the reaction was finished monitoring by TLC. Then the cloudy mixture was filtered to give a yellow filter cake until it was cooled to room temperature. The resulted solid was washed with 1,4-dioxane and water, and dried under vacuum to afford a yellow solid (2.46 g, yield 90%). MS (ESI^+): $[\text{M} + \text{H}]^+$ calculated for $\text{C}_9\text{H}_6\text{NBrO}$, 222.9633; found, 223.9712. ^1H NMR (400 MHz, $\text{DMSO}-d_6$) δ 12.06 (s, 1H), 7.82 (dd, $J = 8.1, 1.0$ Hz, 1H), 7.61 (ddd, $J = 8.4, 7.3, 1.3$ Hz, 1H), 7.36 (d, $J = 8.2$ Hz, 1H), 7.33 – 7.28 (m, 1H), 7.03 (d, $J = 1.5$ Hz, 1H).

tert-butyl (4-((2-oxo-1,2-dihydroquinolin-4-yl)amino)phenyl)carbamate (4). Compound 3 (2.24 g, 0.01 mol), potassium tert-butoxide (2.80 g, 0.025 mol) and tert-butyl (4-aminophenyl) carbamate (2.49 g, 0.012 mol) were suspended in dry 1,4-dioxane (50 ml). Then a solution of $\text{Pd}_2(\text{dba})_3$ (0.915 g, 1 mmol) and Xantphos (2.02 g, 3.5 mmol) in dry 1,4-dioxane (10 ml), were added to the mixture and the

round-bottom flask was sealed off with nitrogen. The resulting suspension was stirred at 100 °C under nitrogen for 16 h. The mixture was filtered to give a brown filter liquor, then removed under reduced pressure to afford a crude product which was purified by silica gel column chromatography (DCM/MeOH=12:1) to afford 2.32 g (yield 66%) of the desired product as a brown solid. MS (ESI⁺): [M + H]⁺ calculated for C₂₀H₂₁N₃O₃, 351.1583; found, 352.1665. ¹H NMR (400 MHz, DMSO-*d*₆) δ 10.95 (s, 1H), 9.41 (s, 1H), 8.52 (s, 1H), 8.10 (d, *J* = 7.9 Hz, 1H), 7.57 – 7.45 (m, 3H), 7.29 – 7.23 (m, 1H), 7.23 – 7.13 (m, 3H), 5.46 (d, *J* = 0.9 Hz, 1H), 1.49 (s, 9H).

4-((4-aminophenyl)amino)quinolin-2(1H)-one (5). Compound 4 (2.2 g, 6.26 mmol) was put in a round-bottom flask and trifluoroacetic acid (20 ml) was slowly poured into the flask. The reaction mixture was stirred at room temperature overnight. The solution was removed under reduced pressure to afford an oil-like crude product. NaHCO₃ saturated solution (50 ml) was then added to the crude product, which was then extracted with DCM (20 ml) three times, washed with brine and dried over Na₂SO₄. The solvent was removed by evaporation under vacuum to a brown solid as compound 5 (1.51 g, yield 92%). MS (ESI⁺): [M + H]⁺ calculated for C₁₅H₁₃N₃O, 251.1059; found, 252.1143. ¹H NMR (400 MHz, DMSO-*d*₆) δ 10.82 (s, 1H), 8.32 (s, 1H), 8.09 (d, *J* = 7.8 Hz, 1H), 7.46 (dd, *J* = 11.3, 4.1 Hz, 1H), 7.28 – 7.21 (m, 1H), 7.18 – 7.08 (m, 1H), 6.94 (d, *J* = 8.6 Hz, 2H), 6.67 – 6.60 (m, 2H), 5.25 (s, 1H), 5.14 (s, 2H).

2-chloro-N-(4-((2-oxo-1,2-dihydroquinolin-4-yl)amino)phenyl)acetamide (6).

Chloroacetyl chloride (0.80 g, 7.17 mmol) was added dropwise to a mixture of

compound **5** (1.5 g, 6 mmol) and triethylamine (1.21 g, 12 mmol) in freshly distilled DMF (50 ml) in an oven-dried round bottom flask at 0-5°C for 30 minutes and at room temperature for further 3 h. After the reaction monitored by TLC was over, water (150 ml) was added to the reaction mixture under stirring, and the suspended mixture was filtered to give a brown solid as compound **6** (1.86 g, yield 95%). MS (ESI⁺): [M + H]⁺ calculated for C₁₇H₁₄N₃O₂Cl, 327.0775; found, 328.0852. ¹H NMR (400 MHz, DMSO-*d*₆) δ 11.02 (s, 1H), 10.89 (s, 1H), 8.71 (s, 1H), 8.19 (d, *J* = 8.1 Hz, 1H), 7.72 (d, *J* = 8.6 Hz, 2H), 7.50 (t, *J* = 7.6 Hz, 2H), 7.33 – 7.27 (m, 3H), 7.16 (t, *J* = 7.5 Hz, 1H), 5.58 (s, 1H), 4.35 (s, 2H).

General procedure for synthesis of compounds 7a-7l. Compound **6** (1.0 equiv) with catalytic equivalent KI was dissolved in freshly distilled DMF in an oven-dried round bottom flask. Different aliphatic amines (3.0 equiv) was added dropwise. The reaction mixture was stirred at room temperature for about 4 hours. After the reaction monitored by TLC was over, water was added to the reaction mixture under stirring, and the suspended mixture was filtered. The crude residue was purified by column chromatography on silica gel to obtain the final products.

N-(4-((2-oxo-1,2-dihydroquinolin-4-yl)amino)phenyl)-2-(pyrrolidin-1-yl)acetamide (**7a**). Yield: 62%; white solid; MS (ESI⁺): [M + H]⁺ calculated for C₂₁H₂₂N₄O₂, 362.1743; found, 363.1821; ¹H NMR (400 MHz, DMSO-*d*₆) δ 10.96 (s, 1H), 9.74 (s, 1H), 8.55 (s, 1H), 8.10 (d, *J* = 7.8 Hz, 1H), 7.70 (d, *J* = 8.8 Hz, 2H), 7.49 (t, *J* = 7.3 Hz, 1H), 7.26 (t, *J* = 8.8 Hz, 3H), 7.17 (t, *J* = 7.6 Hz, 1H), 5.54 (s, 1H), 3.25 (s, 2H), 2.60 (d, *J* = 5.3 Hz, 4H), 1.80 – 1.72 (m, 4H). ¹³C NMR (101 MHz, DMSO-*d*₆) δ 169.18, 163.40,

533 151.01, 139.84, 135.93, 135.55, 130.97, 125.13, 122.82, 121.22, 120.87, 116.13,
 534 114.29, 94.12, 60.02, 54.19, 23.95.

535 *N*-(4-((2-oxo-1,2-dihydroquinolin-4-yl)amino)phenyl)-2-(piperidin-1-yl)aceta-mi
 536 *de* (**7b**). Yield: 84%; white solid; MS (ESI⁺): [M + H]⁺ calculated for C₂₂H₂₄N₄O₂,
 537 376.1899; found, 377.1971; ¹H NMR (400 MHz, DMSO-*d*₆) δ 10.97 (s, 1H), 9.71 (s,
 538 1H), 8.56 (s, 1H), 8.11 (d, *J* = 7.8 Hz, 1H), 7.69 (d, *J* = 8.8 Hz, 2H), 7.49 (dd, *J* = 11.3,
 539 4.1 Hz, 1H), 7.27 (t, *J* = 7.6 Hz, 3H), 7.20 – 7.13 (m, 1H), 5.55 (s, 1H), 3.07 (s, 2H),
 540 2.50 (td, *J* = 3.9, 2.1 Hz, 4H), 1.62 – 1.53 (m, 4H), 1.45 – 1.37 (m, 2H). ¹³C NMR (101
 541 MHz, DMSO-*d*₆) δ 168.97, 163.41, 150.99, 139.84, 135.76, 135.63, 130.97, 125.15,
 542 122.83, 121.23, 120.81, 116.14, 114.30, 94.14, 63.14, 54.58, 25.94, 24.03.

543 *2-morpholino-N*-(4-((2-oxo-1,2-dihydroquinolin-4-yl)amino)phenyl)acetamide
 544 (**7c**). Yield: 80%; white solid; MS (ESI⁺): [M + H]⁺ calculated for C₂₁H₂₂N₄O₃,
 545 378.1692; found, 379.1779; ¹H NMR (400 MHz, MeOD) δ 8.08 (d, *J* = 7.9 Hz, 1H),
 546 7.68 (d, *J* = 8.8 Hz, 2H), 7.57 (t, *J* = 7.2 Hz, 1H), 7.40 – 7.26 (m, 4H), 5.86 (s, 1H), 3.82
 547 – 3.74 (m, 4H), 3.20 (s, 2H), 2.65 – 2.58 (m, 4H).

548 *2*-(4-methylpiperidin-1-yl)-*N*-(4-((2-oxo-1,2-dihydroquinolin-4-yl)amino)phenyl)
 549 *acetamide* (**7d**). Yield: 75%; white solid; MS (ESI⁺): [M + H]⁺ calculated for
 550 C₂₃H₂₆N₄O₂, 390.2056; found, 391.2129; ¹H NMR (400 MHz, DMSO-*d*₆) δ 10.98 (s,
 551 1H), 9.71 (s, 1H), 8.57 (s, 1H), 8.12 (d, *J* = 8.0 Hz, 1H), 7.70 (d, *J* = 8.7 Hz, 2H), 7.50 (t,
 552 *J* = 7.4 Hz, 1H), 7.27 (t, *J* = 8.1 Hz, 3H), 7.18 (t, *J* = 7.5 Hz, 1H), 5.56 (s, 1H), 3.10 (s,
 553 2H), 2.85 (d, *J* = 11.4 Hz, 2H), 2.14 (t, *J* = 10.7 Hz, 2H), 1.60 (d, *J* = 11.4 Hz, 2H), 1.33
 554 – 1.21 (m, 3H), 0.92 (d, *J* = 6.0 Hz, 3H).

2-(4-methylpiperazin-1-yl)-N-(4-((2-oxo-1,2-dihydroquinolin-4-yl)amino)phenyl)acetamide (**7e**). Yield: 66%; white solid; MS (ESI⁺): [M + H]⁺ calculated for C₂₂H₂₅N₅O₂, 391.2008; found, 392.2183; ¹H NMR (400 MHz, DMSO-*d*₆) δ 10.96 (s, 1H), 9.72 (s, 1H), 8.55 (s, 1H), 8.10 (d, *J* = 7.9 Hz, 1H), 7.68 (d, *J* = 8.8 Hz, 2H), 7.49 (t, *J* = 7.2 Hz, 1H), 7.26 (dd, *J* = 8.1, 6.2 Hz, 3H), 7.17 (t, *J* = 7.6 Hz, 1H), 5.54 (d, *J* = 1.3 Hz, 1H), 3.12 (s, 2H), 2.51 (s, 4H), 2.36 (d, *J* = 24.3 Hz, 4H), 2.18 (s, 3H).

2-(4-ethylpiperazin-1-yl)-N-(4-((2-oxo-1,2-dihydroquinolin-4-yl)amino)phenyl)acetamide (**7f**). Yield: 48%; white solid; MS (ESI⁺): [M + H]⁺ calculated for C₂₃H₂₇N₅O₂, 405.2165; found, 406.2238; ¹H NMR (400 MHz, DMSO-*d*₆) δ 10.97 (s, 1H), 9.74 (s, 1H), 8.56 (s, 1H), 8.11 (d, *J* = 8.0 Hz, 1H), 7.69 (d, *J* = 8.5 Hz, 2H), 7.50 (t, *J* = 7.4 Hz, 1H), 7.27 (t, *J* = 7.4 Hz, 3H), 7.18 (t, *J* = 7.4 Hz, 1H), 5.55 (s, 1H), 3.13 (s, 2H), 2.52 (s, 4H), 2.45 (s, 4H), 2.34 (t, *J* = 14.1, 7.0 Hz, 2H), 1.00 (t, *J* = 7.1 Hz, 3H).

2-(4-acetylpiperazin-1-yl)-N-(4-((2-oxo-1,2-dihydroquinolin-4-yl)amino)phenyl)acetamide (**7g**). Yield: 80%; white solid; MS (ESI⁺): [M + H]⁺ calculated for C₂₃H₂₅N₅O₃, 419.1957; found, 420.2037; ¹H NMR (400 MHz, DMSO-*d*₆) δ 10.98 (s, 1H), 9.82 (s, 1H), 8.57 (s, 1H), 8.11 (d, *J* = 7.7 Hz, 1H), 7.70 (d, *J* = 8.8 Hz, 2H), 7.55 – 7.44 (m, 1H), 7.27 (dd, *J* = 7.9, 5.2 Hz, 3H), 7.20 – 7.13 (m, 1H), 5.55 (s, 1H), 3.50 (dd, *J* = 10.1, 5.8 Hz, 4H), 3.18 (s, 2H), 2.58 – 2.52 (m, 2H), 2.50 – 2.46 (m, 2H), 2.00 (s, 3H). ¹³C NMR (101 MHz, DMSO-*d*₆) δ 168.66, 168.49, 163.39, 150.98, 139.84, 135.77, 135.69, 130.98, 125.13, 122.83, 121.23, 120.95, 116.13, 114.29, 94.17, 61.92, 52.89, 46.07, 21.64.

2-(4-(dimethylamino)piperidin-1-yl)-N-(4-((2-oxo-1,2-dihydroquinolin-4-yl)

577 *amino)phenyl)acetamide (7h)*. Yield: 45%; white solid; MS (ESI⁺): [M + H]⁺ calculated
578 for C₂₄H₂₉O₅N₂, 419.2321; found, 420.2393; ¹H NMR (400 MHz, DMSO-*d*₆) δ 10.96 (s,
579 1H), 9.78 (s, 1H), 8.57 (s, 1H), 8.12 (d, *J* = 8.0 Hz, 1H), 7.70 (d, *J* = 8.7 Hz, 2H), 7.50 (t,
580 *J* = 7.6 Hz, 1H), 7.27 (t, *J* = 7.6 Hz, 3H), 7.18 (t, *J* = 7.6 Hz, 1H), 5.55 (s, 1H), 3.16 (s,
581 2H), 3.02 – 2.95 (m, 2H), 2.87 – 2.77 (m, 1H), 2.57 (s, 6H), 2.22 (t, *J* = 11.2 Hz, 2H),
582 1.89 (d, *J* = 11.7 Hz, 2H), 1.73 – 1.60 (m, 2H). ¹³C NMR (101 MHz, DMSO-*d*₆) δ
583 168.78, 163.50, 151.07, 139.70, 135.71, 135.63, 131.08, 125.14, 122.92, 121.36,
584 120.94, 116.15, 114.26, 94.08, 62.32, 61.68, 52.23, 40.61, 26.87.

585 *tert-butyl 4-(2-oxo-2-((4-((2-oxo-1,2-dihydroquinolin-4-yl)amino)phenyl)amino)*
586 *ethyl)piperazine-1-carboxylate (7i)*. Yield: 82%; white solid; MS (ESI⁺): [M + H]⁺
587 calculated for C₂₆H₃₁O₅N₄, 477.2376; found, 500.2272; ¹H NMR (400 MHz, DMSO-*d*₆)
588 δ 11.00 (s, 1H), 9.93 (s, 1H), 8.65 (s, 1H), 8.16 (d, *J* = 8.1 Hz, 1H), 7.71 (d, *J* = 8.8 Hz,
589 2H), 7.50 (t, *J* = 7.7 Hz, 1H), 7.28 (dd, *J* = 11.4, 8.6 Hz, 3H), 7.17 (t, *J* = 7.3 Hz, 1H),
590 5.56 (s, 1H), 3.39 (s, 4H), 3.19 (s, 2H), 2.51 – 2.47 (m, 4H), 1.41 (s, 9H). ¹³C NMR (101
591 MHz, DMSO-*d*₆) δ 168.53, 163.44, 154.36, 151.04, 139.80, 135.77, 135.68, 130.97,
592 125.09, 122.95, 121.25, 120.89, 116.14, 114.31, 94.09, 79.30, 61.94, 52.89, 28.54.

593 *N-(4-((2-oxo-1,2-dihydroquinolin-4-yl)amino)phenyl)-2-((tetrahydro-2H-pyran-4*
594 *-yl)amino)acetamide (7j)*. Yield: 57%; white solid; MS (ESI⁺): [M + H]⁺ calculated for
595 C₂₂H₂₄N₄O₃, 392.1848; found, 393.1926; ¹H NMR (400 MHz, DMSO-*d*₆) δ 10.96 (s,
596 1H), 9.87 (s, 1H), 8.55 (s, 1H), 8.10 (d, *J* = 7.8 Hz, 1H), 7.69 (d, *J* = 8.8 Hz, 2H), 7.49 (t,
597 *J* = 7.2 Hz, 1H), 7.26 (dd, *J* = 7.9, 5.2 Hz, 3H), 7.17 (t, *J* = 7.6 Hz, 1H), 5.54 (s, 1H),
598 3.84 (dt, *J* = 11.4, 3.4 Hz, 2H), 3.33 (s, 2H), 3.28 (dd, *J* = 11.5, 2.1 Hz, 2H), 2.68 – 2.58

(m, 1H), 1.77 (d, $J = 12.5$ Hz, 2H), 1.31 (ddd, $J = 14.5, 11.5, 3.7$ Hz, 2H). ^{13}C NMR (101 MHz, DMSO- d_6) δ 170.94, 163.42, 151.01, 139.83, 135.85, 135.53, 130.99, 125.26, 122.82, 121.25, 120.52, 116.15, 114.29, 94.11, 66.22, 53.84, 50.16, 33.56.

2-(diethylamino)-N-(4-((2-oxo-1,2-dihydroquinolin-4-yl)amino)phenyl)acetamide (7k). Yield: 45%; white solid; MS (ESI $^+$): $[\text{M} + \text{H}]^+$ calculated for $\text{C}_{21}\text{H}_{24}\text{N}_4\text{O}_2$, 364.1899; found, 365.1974; ^1H NMR (400 MHz, MeOD) δ 8.13 – 8.08 (m, 1H), 7.69 (d, $J = 8.8$ Hz, 2H), 7.58 (t, $J = 7.7$ Hz, 1H), 7.41 – 7.26 (m, 4H), 5.86 (s, 1H), 3.49 (s, 2H), 2.88 (q, $J = 7.2$ Hz, 4H), 1.20 (t, $J = 7.2$ Hz, 6H).

2-(ethylamino)-N-(4-((2-oxo-1,2-dihydroquinolin-4-yl)amino)phenyl)acetamide (7l). Yield: 47%; white solid; MS (ESI $^+$): $[\text{M} + \text{H}]^+$ calculated for $\text{C}_{19}\text{H}_{20}\text{O}_4\text{N}_2$, 336.1586; found, 337.1661; ^1H NMR (400 MHz, DMSO- d_6) δ 10.98 (s, 1H), 10.35 (s, 1H), 8.58 (s, 1H), 8.11 (d, $J = 8.1$ Hz, 1H), 7.66 (d, $J = 8.7$ Hz, 2H), 7.51 (t, $J = 7.6$ Hz, 1H), 7.29 (t, $J = 9.0$ Hz, 3H), 7.18 (t, $J = 7.6$ Hz, 1H), 5.58 (s, 1H), 3.80 (s, 2H), 2.94 (q, $J = 7.1$ Hz, 2H), 1.18 (dd, $J = 9.0, 5.4$ Hz, 3H).

General procedure for synthesis of diphenyl sulfide derivative.
2,4-dichloroquinoline (8). 4-hydroxyquinolin-2(1H)-one (10 g, 0.062 mol) was first put in a round-bottom flask and POCl_3 (40 ml) was slowly pour into the flask in 1 hour under stirring. After stirring for another 30 minutes, the black mixture was heated to 100 $^\circ\text{C}$ and stirred for another 6 hours. When it was cooled to room temperature, the solution was removed under reduced pressure to afford an oil-like black product. Ice NaHCO_3 saturated solution was added to the mixture slowly until no bubbles formed. Ethyl acetate (100 ml) was added subsequently. The organic phase was separated, dried

over anhydrous Na_2SO_4 , and then evaporated. Petroleum ether (200 ml) was added to the crude product and stirred about 30 minutes. The mixture was filtered, then the filter liquor was collected and dried in vacuum to obtain compound 8 as a yellow solid (7.9 g, 65% yield) without further purification. MS (ESI^+): $[\text{M} + \text{H}]^+$ calculated for $\text{C}_9\text{H}_5\text{NCl}_2$, 196.9799; found, 197.9877.

4-chloroquinolin-2(1H)-one (9). Compound 8 (7.0 g, 0.035 mol) was dissolved in 1,4-dioxane (30 ml) in a round bottom flask and heated. Hydrochloric acid which consists of 60% water (30 ml) then was added to the mixture after it was heated to 90°C . The reaction mixture was stirred at 90°C after the reaction was finished monitored by TLC. Then the cloudy mixture was filtered to give a yellow filter cake until it was cooled to room temperature. The resulted solid was washed with 1,4-dioxane and water, and dried under vacuum to afford the yellow solid (5.69 g, yield 90%). MS (ESI^+): $[\text{M} + \text{H}]^+$ calculated for $\text{C}_9\text{H}_6\text{NOCl}$, 179.0138; found, 180.0146. ^1H NMR (400 MHz, $\text{DMSO}-d_6$) δ 12.05 (s, 1H), 7.81 (dd, $J = 8.1, 1.0$ Hz, 1H), 7.60 (ddd, $J = 8.4, 7.3, 1.3$ Hz, 1H), 7.35 (d, $J = 8.2$ Hz, 1H), 7.32 – 7.27 (m, 1H), 7.03 (s, 1H).

4-((4-aminophenyl)thio)quinolin-2(1H)-one (10). Compound 9 (5.0 g, 0.03 mol), 4-aminobenzenethiol (7.0 g, 0.06 mol) and K_2CO_3 (12.42 g, 0.09 mol) were put in a round bottom flask, then DMF (200 ml) was added. When the mixture was heated to 130°C , 4-chloroquinolin-2(1H)-one (5.37 g, 0.03 mol) was added and stirred for another 6 hours. After the reaction was finished monitored by TLC, the mixture was cooled to room temperature and 400 ml water was added to form a suspending mixture. Then solid was collected through a filter. After purified by silica gel column chromatography

(DCM/MeOH=24:1), brown solid was afforded as compound 10 (4.66 g, yield 58%).

MS (ESI⁺): [M + H]⁺ calculated for C₁₅H₁₂N₂OS, 268.0670; found, 269.0678. ¹H NMR (400 MHz, DMSO-*d*₆) δ 11.53 (s, 1H), 7.82 (d, *J* = 7.6 Hz, 1H), 7.59 – 7.52 (m, 1H), 7.33 (d, *J* = 8.1 Hz, 1H), 7.23 (t, *J* = 7.7 Hz, 3H), 6.72 (d, *J* = 8.5 Hz, 2H), 5.74 (s, 2H), 5.56 (s, 1H).

2-chloro-N-(4-((2-oxo-1,2-dihydroquinolin-4-yl)thio)phenyl)acetamide (11).

Compound 11 was prepared as the same method as compound 6; brown solid, yield 95%. MS (ESI⁺): [M + H]⁺ calculated for C₁₇H₁₃N₂O₂SCl, 344.0386; found, 345.0392. ¹H NMR (400 MHz, DMSO-*d*₆) δ 11.65 (s, 1H), 10.76 (s, 1H), 7.84 (dd, *J* = 8.3, 3.2 Hz, 3H), 7.67 – 7.54 (m, 3H), 7.36 (d, *J* = 8.2 Hz, 1H), 7.26 (t, *J* = 7.5 Hz, 1H), 5.58 (s, 1H), 4.34 (s, 2H).

General procedure for synthesis of compounds 12a-12l was same as compounds 7a-7l.

N-(4-((2-oxo-1,2-dihydroquinolin-4-yl)thio)phenyl)-2-(pyrrolidin-1-yl)acetamide (12a). Yield: 71%; white solid; MS (ESI⁺): [M + H]⁺ calculated for C₂₁H₂₁N₃O₂S, 379.1354; found, 380.1424; ¹H NMR (400 MHz, DMSO-*d*₆) δ 11.62 (s, 1H), 10.04 (s, 1H), 7.87 (dd, *J* = 15.0, 8.2 Hz, 3H), 7.58 (t, *J* = 7.8 Hz, 3H), 7.35 (d, *J* = 8.0 Hz, 1H), 7.27 (d, *J* = 8.0 Hz, 1H), 5.57 (s, 1H), 3.30 (s, 2H), 2.61 (s, 4H), 1.77 (dd, *J* = 6.5, 3.2 Hz, 4H). ¹³C NMR (101 MHz, DMSO-*d*₆) δ 169.82, 162.77, 160.67, 152.46, 141.33, 138.48, 137.02, 131.70, 123.73, 122.42, 121.39, 120.86, 117.39, 116.33, 115.55, 60.07, 54.16, 23.95.

N-(4-((2-oxo-1,2-dihydroquinolin-4-yl)thio)phenyl)-2-(piperidin-1-yl)acetamide

665 (12b). Yield: 75%; white solid; MS (ESI⁺): [M + H]⁺ calculated for C₂₂H₂₃N₃O₂S,
 666 393.1511; found, 394.1588; ¹H NMR (400 MHz, DMSO-*d*₆) δ 11.63 (s, 1H), 9.99 (s,
 667 1H), 7.90 – 7.82 (m, 3H), 7.59 (ddd, *J* = 10.9, 6.2, 1.6 Hz, 3H), 7.35 (d, *J* = 7.7 Hz, 1H),
 668 7.29 – 7.24 (m, 1H), 5.58 (s, 1H), 3.12 (s, 2H), 2.50 – 2.45 (m, 4H), 1.58 (dt, *J* = 11.0,
 669 5.7 Hz, 4H), 1.42 (d, *J* = 5.0 Hz, 2H). ¹³C NMR (101 MHz, DMSO-*d*₆) δ 169.68, 160.69,
 670 152.48, 141.15, 138.46, 137.06, 131.72, 123.74, 122.45, 121.35, 120.96, 117.39,
 671 116.34, 115.54, 63.18, 54.53, 25.90, 24.02.

672 *2-morpholino-N-(4-((2-oxo-1,2-dihydroquinolin-4-yl)thio)phenyl)acetamide* (12c).

673 Yield: 68%; white solid; MS (ESI⁺): [M + H]⁺ calculated for C₂₁H₂₁N₃O₃S, 395.1304;
 674 found, 396.1383; ¹H NMR (400 MHz, DMSO-*d*₆) δ 11.59 (s, 1H), 10.03 (s, 1H), 7.82
 675 (dd, *J* = 11.4, 8.6 Hz, 3H), 7.55 (dd, *J* = 12.6, 8.0 Hz, 3H), 7.31 (d, *J* = 8.2 Hz, 1H), 7.22
 676 (t, *J* = 7.6 Hz, 1H), 5.53 (s, 1H), 3.73 – 3.53 (m, 4H), 3.15 (s, 2H), 2.47 (s, 4H). ¹³C
 677 NMR (101 MHz, DMSO-*d*₆) δ 169.16, 160.70, 152.49, 141.16, 138.46, 137.05, 131.71,
 678 123.74, 122.45, 121.42, 121.03, 117.40, 116.35, 115.52, 66.55, 62.56, 53.62.

679 *2-(4-methylpiperidin-1-yl)-N-(4-((2-oxo-1,2-dihydroquinolin-4-yl)thio)phenyl)*

680 *acetamide* (12d). Yield: 81%; white solid; MS (ESI⁺): [M + H]⁺ calculated for
 681 C₂₃H₂₅N₃O₂S, 407.1667; found, 408.1745; ¹H NMR (400 MHz, DMSO-*d*₆) δ 11.63 (s,
 682 1H), 9.98 (s, 1H), 7.86 (dd, *J* = 10.6, 8.0 Hz, 3H), 7.62 – 7.55 (m, 3H), 7.35 (d, *J* = 7.7
 683 Hz, 1H), 7.29 – 7.23 (m, 1H), 5.57 (d, *J* = 1.1 Hz, 1H), 3.13 (s, 2H), 2.85 (d, *J* = 11.6 Hz,
 684 2H), 2.14 (t, *J* = 10.4 Hz, 2H), 1.60 (d, *J* = 10.2 Hz, 2H), 1.36 – 1.21 (m, 3H), 0.92 (d, *J*
 685 = 6.1 Hz, 3H). ¹³C NMR (101 MHz, DMSO-*d*₆) δ 169.71, 160.69, 152.48, 141.15,
 686 138.46, 137.05, 131.71, 123.74, 122.45, 121.36, 120.96, 117.40, 116.34, 115.53, 62.80,

53.93, 34.26, 30.32, 22.27.

2-(4-methylpiperazin-1-yl)-N-(4-((2-oxo-1,2-dihydroquinolin-4-yl)thio)phenyl)

acetamide (12e). Yield: 70%; white solid; MS (ESI⁺): [M + H]⁺ calculated for C₂₂H₂₄N₄O₂S, 408.1620; found, 409.1700; ¹H NMR (400 MHz, DMSO-*d*₆) δ 11.67 (s, 1H), 10.19 (s, 1H), 7.86 (dd, *J* = 18.9, 8.2 Hz, 3H), 7.58 (t, *J* = 8.3 Hz, 3H), 7.38 (d, *J* = 8.2 Hz, 1H), 7.25 (t, *J* = 7.6 Hz, 1H), 5.57 (s, 1H), 3.17 (d, *J* = 7.6 Hz, 2H), 2.54 (s, 4H), 2.38 (s, 4H), 2.18 (s, 3H).

2-(4-ethylpiperazin-1-yl)-N-(4-((2-oxo-1,2-dihydroquinolin-4-yl)thio)phenyl)

acetamide (12f). Yield: 68%; white solid; MS (ESI⁺): [M + H]⁺ calculated for C₂₃H₂₆N₄O₂S, 422.1776; found, 423.1850; ¹H NMR (400 MHz, DMSO-*d*₆) δ 11.63 (s, 1H), 10.02 (s, 1H), 7.86 (t, *J* = 8.5 Hz, 3H), 7.65 – 7.52 (m, 3H), 7.35 (d, *J* = 8.1 Hz, 1H), 7.26 (t, *J* = 7.6 Hz, 1H), 5.57 (s, 1H), 3.17 (s, 2H), 2.55 (s, 4H), 2.44 (s, 4H), 2.34 (q, *J* = 7.1 Hz, 2H), 1.00 (t, *J* = 7.2 Hz, 3H). ¹³C NMR (101 MHz, DMSO-*d*₆) δ 169.35, 160.70, 152.50, 141.15, 138.44, 137.06, 131.72, 123.74, 122.46, 121.35, 120.99, 117.39, 116.35, 115.51, 62.33, 53.22, 52.62, 52.04, 12.42.

2-(4-acetylpiperazin-1-yl)-N-(4-((2-oxo-1,2-dihydroquinolin-4-yl)thio)phenyl)

acetamide (12g). Yield: 72%; white solid; MS (ESI⁺): [M + H]⁺ calculated for C₂₃H₂₄N₄O₃S, 436.1569; found, 437.1685; ¹H NMR (400 MHz, DMSO-*d*₆) δ 11.63 (s, 1H), 10.09 (s, 1H), 7.86 (dd, *J* = 14.6, 8.3 Hz, 3H), 7.64 – 7.55 (m, 3H), 7.35 (d, *J* = 8.2 Hz, 1H), 7.25 (dd, *J* = 11.3, 4.1 Hz, 1H), 5.57 (s, 1H), 3.51 (dd, *J* = 10.1, 6.2 Hz, 4H), 3.23 (s, 2H), 2.59 – 2.53 (m, 2H), 2.49 (d, *J* = 9.3 Hz, 2H), 2.00 (s, 3H).

2-(4-(dimethylamino)piperidin-1-yl)-N-(4-((2-oxo-1,2-dihydroquinolin-4-yl)thio)

phenyl)acetamide (12h). Yield: 68%; white solid; MS (ESI⁺): [M + H]⁺ calculated for C₂₂H₂₈N₄O₂S, 436.1933; found, 437.2006; ¹H NMR (400 MHz, DMSO-*d*₆) δ 11.64 (s, 1H), 10.06 (s, 1H), 7.87 (dd, *J* = 12.9, 8.5 Hz, 3H), 7.64 – 7.54 (m, 3H), 7.36 (d, *J* = 8.2 Hz, 1H), 7.26 (t, *J* = 7.5 Hz, 1H), 5.57 (s, 1H), 3.18 (s, 2H), 2.96 (d, *J* = 11.2 Hz, 2H), 2.52 (s, 1H), 2.37 (s, 6H), 2.19 (t, *J* = 11.2 Hz, 2H), 1.82 (d, *J* = 11.0 Hz, 2H), 1.66 – 1.52 (m, 2H). ¹³C NMR (101 MHz, DMSO-*d*₆) δ 169.53, 160.72, 152.53, 141.17, 138.44, 137.04, 131.72, 123.73, 122.47, 121.42, 121.00, 117.40, 116.36, 115.49, 62.02, 52.62, 41.11, 27.54.

tert-butyl-4-(2-oxo-2-((4-((2-oxo-1,2-dihydroquinolin-4-yl)thio)phenyl)amino)ethyl)piperazine-1-carboxylate (12i). Yield: 88%; white solid; MS (ESI⁺): [M + H]⁺ calculated for C₂₆H₃₀N₄O₄S, 494.1988; found, 495.2078; ¹H NMR (400 MHz, DMSO-*d*₆) δ 11.63 (s, 1H), 10.07 (s, 1H), 7.86 (dd, *J* = 10.9, 8.7 Hz, 3H), 7.59 (dd, *J* = 12.5, 8.0 Hz, 3H), 7.35 (d, *J* = 8.2 Hz, 1H), 7.26 (t, *J* = 7.6 Hz, 1H), 5.57 (s, 1H), 3.40 (m, 4H), 3.21 (s, 2H), 2.49 (m, 4H), 1.41 (s, 9H).

N-(4-((2-oxo-1,2-dihydroquinolin-4-yl)thio)phenyl)-2-((tetrahydro-2H-pyran-4-yl)-amino)acetamide (12j). Yield: 70%; white solid; MS (ESI⁺): [M + H]⁺ calculated for C₂₂H₂₃N₃O₃S, 409.1460; found, 410.1537; ¹H NMR (400 MHz, DMSO-*d*₆) δ 11.63 (s, 1H), 10.16 (s, 1H), 7.85 (dd, *J* = 13.4, 4.8 Hz, 3H), 7.68 – 7.51 (m, 3H), 7.35 (d, *J* = 7.8 Hz, 1H), 7.30 – 7.21 (m, 1H), 5.57 (s, 1H), 3.84 (dt, *J* = 11.4, 3.4 Hz, 2H), 3.38 (s, 2H), 3.28 (m, 3H), 2.64 (ddd, *J* = 14.3, 10.2, 4.0 Hz, 1H), 1.82 – 1.74 (m, 2H), 1.36 – 1.23 (m, 2H). ¹³C NMR (101 MHz, DMSO-*d*₆) δ 171.69, 160.68, 152.48, 141.21, 138.47, 137.14, 131.70, 123.73, 122.43, 121.09, 120.84, 117.39, 116.34, 115.53, 66.21, 53.78, 50.27,

33.54.

2-(diethylamino)-N-(4-((2-oxo-1,2-dihydroquinolin-4-yl)thio)phenyl)acetamide

(12k). Yield: 76%; white solid; MS (ESI⁺): [M + H]⁺ calculated for C₂₁H₂₃N₃O₂S, 381.1511; found, 382.1589; ¹H NMR (400 MHz, DMSO-*d*₆) δ 11.63 (s, 1H), 9.95 (s, 1H), 7.87 (dd, *J* = 18.0, 8.4 Hz, 3H), 7.63 – 7.54 (m, 3H), 7.35 (d, *J* = 8.2 Hz, 1H), 7.30 – 7.21 (m, 1H), 5.58 (s, 1H), 3.21 (s, 2H), 2.63 (q, *J* = 7.1 Hz, 4H), 1.04 (t, *J* = 7.1 Hz, 6H). ¹³C NMR (101 MHz, DMSO-*d*₆) δ 170.96, 160.68, 152.45, 141.01, 138.48, 137.06, 131.71, 123.74, 122.43, 121.33, 121.00, 117.40, 116.34, 115.56, 57.89, 48.26, 12.40.

2-(ethylamino)-N-(4-((2-oxo-1,2-dihydroquinolin-4-yl)thio)phenyl)acetamide

(12l). Yield: 73%; white solid; MS (ESI⁺): [M + H]⁺ calculated for C₁₉H₁₉N₃O₂S, 353.1198; found, 354.1278; ¹H NMR (400 MHz, DMSO-*d*₆) δ 11.62 (s, 1H), 10.03 (s, 1H), 7.86 (t, *J* = 9.1 Hz, 3H), 7.67 – 7.54 (m, 3H), 7.35 (d, *J* = 8.1 Hz, 1H), 7.25 (dd, *J* = 11.3, 4.1 Hz, 1H), 5.57 (s, 1H), 3.33 (s, 2H), 2.60 (q, *J* = 7.1 Hz, 2H), 1.06 (t, *J* = 7.1 Hz, 3H). ¹³C NMR (101 MHz, DMSO-*d*₆) δ 171.42, 160.68, 152.47, 141.27, 138.47, 137.13, 131.70, 123.73, 122.43, 121.11, 120.81, 117.39, 116.34, 115.53, 53.13, 43.79, 15.43.

General procedure for synthesis of diphenyl ether derivative.

4-(4-nitrophenoxy)quinolin-2(1H)-one (13). 4-hydroxyquinolin-2(1H)-one (9.66 g, 0.06 mol) and K₂CO₃ (12.42 g, 0.09 mol) were put in a round bottom flask, then DMF (200 ml) was added to heat to 100°. 1-fluoro-4-nitrobenzene (4.23 g, 0.03 mol) was dissolve in another 20 ml DMF, and the solution was added to prepared mixture dropwise in half an hour. The reaction mixture was stirring at room temperature for

another 6 hours. After the reaction was finished monitored by TLC, the mixture was cooled to room temperature and 400 ml water was added to form a suspending mixture. Then solid was collected through a filter. After drying through a vacuum drying oven, a pale yellow solid was afforded as compound 13 (6.11 g, yield 72%). MS (ESI⁺): [M + H]⁺ calculated for C₁₅H₁₀N₂O₄, 282.0641; found, 283.0719. ¹H NMR (400 MHz, DMSO-*d*₆) δ 11.75 (s, 1H), 8.37 (d, *J* = 7.4 Hz, 2H), 7.87 (d, *J* = 6.6 Hz, 1H), 7.62 (s, 1H), 7.55 (d, *J* = 6.8 Hz, 2H), 7.47 – 7.16 (m, 2H), 5.72 (s, 1H).

4-(4-aminophenoxy)quinolin-2(1H)-one (14). Compound 13 (5.66 g, 0.02 mol) and iron Powder (4.48 g, 0.08 mol) was dispersed in 200 ml mixture solution (MeOH/H₂O=9/1), then heated to 85°. Concentrated hydrochloric acid (12 mol/L, 20 ml) was added to it dropwise at 85° during 20 minutes and stirring for another 4 hours. After the reaction was finished monitored by TLC, the mixture was cooled to room temperature and removed under reduced pressure to afford crude product. Then water (100 ml) was added to it and stirring for 10 minutes. Then solid was collected through a filter. After drying through a vacuum drying oven, a gray solid was afforded as compound 14 (4.54 g, yield 90%). MS (ESI⁺): [M + H]⁺ calculated for C₁₅H₁₂N₂O₂, 252.0899; found, 253.0977. ¹H NMR (400 MHz, DMSO-*d*₆) δ 11.60 (s, 1H), 7.95 (d, *J* = 7.7 Hz, 1H), 7.60 (t, *J* = 7.4 Hz, 1H), 7.36 (q, *J* = 8.8 Hz, 5H), 7.25 (t, *J* = 7.3 Hz, 1H), 5.33 (s, 1H).

2-chloro-N-(4-((2-oxo-1,2-dihydroquinolin-4-yl)oxy)phenyl)acetamide (15).

Compound 15 was prepared as the same method as compound 6; brown solid, yield 93%. MS (ESI⁺): [M + H]⁺ calculated for C₁₇H₁₃N₂O₃Cl, 328.0615; found, 329.0711.

¹H NMR (400 MHz, DMSO-*d*₆) δ 11.55 (s, 1H), 10.47 (s, 1H), 7.97 (d, *J* = 8.1 Hz, 1H), 7.74 (d, *J* = 8.6 Hz, 2H), 7.60 (t, *J* = 7.7 Hz, 1H), 7.35 (d, *J* = 8.2 Hz, 1H), 7.26 (dd, *J* = 14.6, 8.0 Hz, 3H), 5.32 (s, 1H), 4.29 (s, 2H).

General procedure for synthesis of compounds 16a-16o was same as compounds 12a-12o.

N-(4-((2-oxo-1,2-dihydroquinolin-4-yl)oxy)phenyl)-2-(pyrrolidin-1-yl)acetamide (16a). Yield: 46%; white solid; MS (ESI⁺): [M + H]⁺ calculated for C₂₁H₂₁N₃O₃, 363.1583; found, 364.1657; ¹H NMR (400 MHz, DMSO-*d*₆) δ 11.54 (s, 1H), 9.87 (s, 1H), 7.98 (d, *J* = 7.9 Hz, 1H), 7.81 (d, *J* = 8.8 Hz, 2H), 7.60 (t, *J* = 7.6 Hz, 1H), 7.36 (d, *J* = 8.2 Hz, 1H), 7.25 (t, *J* = 8.8 Hz, 3H), 5.31 (s, 1H), 3.27 (s, 2H), 2.61 (s, 4H), 1.76 (s, 4H). ¹³C NMR (101 MHz, DMSO-*d*₆) δ 169.37, 163.95, 163.20, 148.76, 139.52, 137.20, 132.04, 122.78, 122.19, 122.00, 121.65, 115.84, 114.61, 100.29, 60.04, 54.19, 23.96.

N-(4-((2-oxo-1,2-dihydroquinolin-4-yl)oxy)phenyl)-2-(piperidin-1-yl)acetamide (16b). Yield: 65%; white solid; MS (ESI⁺): [M + H]⁺ calculated for C₂₂H₂₃N₃O₃, 377.1739; found, 378.1815; ¹H NMR (400 MHz, DMSO-*d*₆) δ 11.54 (s, 1H), 9.83 (s, 1H), 7.98 (d, *J* = 7.9 Hz, 1H), 7.80 (d, *J* = 8.9 Hz, 2H), 7.60 (t, *J* = 7.7 Hz, 1H), 7.36 (d, *J* = 8.2 Hz, 1H), 7.25 (t, *J* = 7.3 Hz, 3H), 5.32 (s, 1H), 3.10 (s, 2H), 2.48 (s, 4H), 1.64 – 1.54 (m, 4H), 1.42 (d, *J* = 4.8 Hz, 2H). ¹³C NMR (101 MHz, DMSO-*d*₆) δ 169.17, 163.94, 163.19, 148.81, 139.53, 137.05, 132.04, 122.78, 122.18, 122.04, 121.60, 115.84, 114.61, 100.31, 63.16, 54.58, 25.92, 24.04.

2-morpholino-N-(4-((2-oxo-1,2-dihydroquinolin-4-yl)oxy)phenyl)acetamide (16c).

Yield: 60%; white solid; MS (ESI⁺): [M + H]⁺ calculated for C₂₁H₂₁N₃O₄, 379.1532;

found, 380.1608; ^1H NMR (400 MHz, $\text{DMSO}-d_6$) δ 11.59 (s, 1H), 10.03 (s, 1H), 7.82 (dd, $J = 11.4, 8.6$ Hz, 3H), 7.55 (dd, $J = 12.6, 8.0$ Hz, 3H), 7.31 (d, $J = 8.2$ Hz, 1H), 7.22 (t, $J = 7.6$ Hz, 1H), 5.53 (s, 1H), 3.73 – 3.53 (m, 4H), 3.15 (s, 2H), 2.47 (s, 4H). ^{13}C NMR (101 MHz, $\text{DMSO}-d_6$) δ 168.66, 163.94, 163.20, 148.85, 139.52, 137.05, 132.05, 122.78, 122.20, 122.05, 121.70, 115.85, 114.60, 100.30, 66.56, 62.53, 53.67.

2-(4-methylpiperidin-1-yl)-N-(4-((2-oxo-1,2-dihydroquinolin-4-yl)oxy)phenyl)-acetamide (16d). Yield: 60%; white solid; MS (ESI^+): $[\text{M} + \text{H}]^+$ calculated for $\text{C}_{23}\text{H}_{25}\text{N}_3\text{O}_3$, 391.1896; found, 392.1976; ^1H NMR (400 MHz, $\text{DMSO}-d_6$) δ 11.55 (s, 1H), 9.82 (s, 1H), 7.97 (d, $J = 7.8$ Hz, 1H), 7.80 (d, $J = 8.8$ Hz, 2H), 7.60 (t, $J = 7.4$ Hz, 1H), 7.36 (d, $J = 8.2$ Hz, 1H), 7.25 (t, $J = 7.1$ Hz, 3H), 5.32 (s, 1H), 3.11 (s, 2H), 2.85 (d, $J = 11.4$ Hz, 2H), 2.13 (t, $J = 11.0$ Hz, 2H), 1.59 (d, $J = 11.1$ Hz, 2H), 1.36 – 1.21 (m, 3H), 0.91 (d, $J = 5.9$ Hz, 3H). ^{13}C NMR (101 MHz, $\text{DMSO}-d_6$) δ 169.19, 163.94, 163.20, 148.81, 139.53, 137.05, 132.03, 122.78, 122.18, 122.04, 121.61, 115.84, 114.61, 100.30, 62.77, 53.97, 34.28, 30.34, 22.27.

2-(4-methylpiperazin-1-yl)-N-(4-((2-oxo-1,2-dihydroquinolin-4-yl)oxy)phenyl)-acetamide (16e). Yield: 45%; white solid; MS (ESI^+): $[\text{M} + \text{H}]^+$ calculated for $\text{C}_{22}\text{H}_{24}\text{N}_4\text{O}_3$, 392.1848; found, 393.1922; ^1H NMR (400 MHz, $\text{DMSO}-d_6$) δ 11.54 (s, 1H), 9.89 (s, 1H), 7.97 (d, $J = 7.3$ Hz, 1H), 7.78 (d, $J = 8.9$ Hz, 2H), 7.64 – 7.56 (m, 1H), 7.36 (d, $J = 8.2$ Hz, 1H), 7.26 (dd, $J = 7.5, 4.9$ Hz, 3H), 5.31 (s, 1H), 3.19 (s, 2H), 2.63 (m, 8H), 2.35 (s, 3H). ^{13}C NMR (101 MHz, $\text{DMSO}-d_6$) δ 168.67, 163.96, 163.25, 148.86, 139.48, 136.99, 132.08, 122.77, 122.25, 122.07, 121.66, 115.86, 114.59, 100.26, 61.56, 54.28, 51.83, 44.91.

819 *2-(4-(tert-butyl)piperazin-1-yl)-N-(4-((2-oxo-1,2-dihydroquinolin-4-yl)oxy)phen*
820 *yl)acetamide (16f)*. Yield: 46%; white solid; MS (ESI⁺): [M + H]⁺ calculated for
821 C₂₅H₃₀N₄O₃, 378.1692; found, 379.1732; ¹H NMR (400 MHz, MeOD) δ 8.11 (d, *JJ* =
822 7.3 Hz, 1H), 7.77 (d, *JJ* = 8.9 Hz, 2H), 7.67 – 7.60 (m, 1H), 7.39 (d, *J* = 8.2 Hz, 1H),
823 7.34 (t, *J* = 7.7 Hz, 1H), 7.23 (d, *J* = 9.0 Hz, 2H), 5.57 (s, 1H), 3.30 (s, 2H), 3.16 (s, 4H),
824 2.86 (s, 4H), 1.32 (s, 9H). ¹³C NMR (101 MHz, DMSO-*d*₆) δ 171.45, 168.71, 163.94,
825 163.19, 148.87, 139.53, 137.06, 132.05, 122.78, 122.19, 122.05, 121.71, 115.84,
826 114.60, 100.32, 61.93, 45.31, 42.01, 10.69, 7.43.

827 *2-(4-(cyclopropanecarbonyl)piperazin-1-yl)-N-(4-((2-oxo-1,2-dihydroquinolin-4-*
828 *yl)oxy)phenyl)acetamide (16g)*. Yield: 66%; white solid; MS (ESI⁺): [M + H]⁺
829 calculated for C₂₅H₂₆N₄O₄, 446.1954; found, 447.1894; ¹H NMR (400 MHz, DMSO-*d*₆)
830 δ 11.54 (s, 1H), 9.93 (s, 1H), 7.97 (d, *J* = 7.6 Hz, 1H), 7.80 (d, *J* = 8.1 Hz, 2H), 7.59 (d,
831 *J* = 7.2 Hz, 1H), 7.35 (d, *J* = 7.9 Hz, 1H), 7.25 (d, *J* = 7.4 Hz, 3H), 5.31 (s, 1H), 3.75 (s,
832 2H), 3.55 (s, 2H), 3.21 (s, 2H), 2.58 (s, 2H), 2.50 – 2.44 (m, 2H), 1.97 (s, 1H), 0.81 –
833 0.58 (m, 4H). ¹³C NMR (101 MHz, DMSO-*d*₆) δ 168.70, 168.63, 163.95, 163.22,
834 148.87, 139.52, 137.05, 132.05, 122.78, 122.19, 122.05, 121.72, 115.85, 114.61,
835 100.30, 61.92, 53.32, 46.05, 21.64.

836 *2-(4-(dimethylamino)piperidin-1-yl)-N-(4-((2-oxo-1,2-dihydroquinolin-4-yl)oxy)*
837 *phenyl)acetamide (16h)*. Yield: 41%; white solid; MS (ESI⁺): [M + H]⁺ calculated for
838 C₂₆H₂₈N₄O₃, 420.2161; found, 421.2237; ¹H NMR (400 MHz, DMSO-*d*₆) δ 11.54 (s,
839 1H), 9.84 (s, 1H), 7.97 (d, *J* = 8.0 Hz, 1H), 7.79 (d, *J* = 8.8 Hz, 2H), 7.60 (t, *J* = 7.6 Hz,
840 1H), 7.35 (d, *J* = 8.2 Hz, 1H), 7.25 (t, *J* = 7.2 Hz, 3H), 5.31 (s, 1H), 3.12 (s, 2H), 2.92 (d,

841 $J = 11.5$ Hz, 2H), 2.51 (m, 1H), 2.26 (s, 6H), 2.16 (t, $J = 11.2$ Hz, 3H), 1.76 (d, $J = 11.7$
 842 Hz, 2H), 1.54 (dd, $J = 20.4, 11.4$ Hz, 2H). ^{13}C NMR (101 MHz, DMSO- d_6) δ 169.00,
 843 163.95, 163.20, 148.84, 139.52, 137.06, 132.06, 122.78, 122.21, 122.05, 121.69,
 844 115.86, 114.60, 100.28, 62.08, 50.80, 41.09, 25.55.

845 *tert-butyl 4-(2-oxo-2-((4-((2-oxo-1,2-dihydroquinolin-4-yl)oxy)phenyl)amino)*
 846 *ethyl)piperazine-1-carboxylate (16i)*. Yield: 60%; white solid; MS (ESI $^+$): $[\text{M} + \text{H}]^+$
 847 calculated for $\text{C}_{26}\text{H}_{30}\text{N}_4\text{O}_5$, 478.2216; found, 479.2274 ; ^1H NMR (400 MHz,
 848 DMSO- d_6) δ 11.54 (s, 1H), 9.90 (s, 1H), 7.97 (d, $J = 8.5$ Hz, 1H), 7.79 (d, $J = 8.9$ Hz,
 849 2H), 7.62 – 7.56 (m, 1H), 7.35 (d, $J = 8.2$ Hz, 1H), 7.25 (dd, $J = 8.1, 4.1$ Hz, 3H), 5.30 (s,
 850 1H), 3.39 (m, 4H), 3.18 (s, 2H), 2.49 (m, 4H), 1.40 (s, 9H). ^{13}C NMR (101 MHz,
 851 DMSO- d_6) δ 168.69, 163.94, 163.21, 154.34, 148.86, 139.52, 137.04, 132.03, 122.78,
 852 122.18, 122.04, 121.69, 115.85, 114.60, 100.30, 79.27, 62.01, 52.92, 28.54.

853 *N-(4-((2-oxo-1,2-dihydroquinolin-4-yl)oxy)phenyl)-2-((tetrahydro-2H-pyran-4-yl*
 854 *)amino)acetamide (16j)*. Yield: 45%; white solid; MS (ESI $^+$): $[\text{M} + \text{H}]^+$ calculated for
 855 $\text{C}_{22}\text{H}_{23}\text{N}_3\text{O}_4$, 393.1689; found, 394.1782 ; ^1H NMR (400 MHz, DMSO- d_6) δ 11.54 (s,
 856 1H), 9.98 (s, 1H), 7.97 (d, $J = 7.5$ Hz, 1H), 7.78 (d, $J = 8.9$ Hz, 2H), 7.59 (t, $J = 7.2$ Hz,
 857 1H), 7.35 (d, $J = 8.2$ Hz, 1H), 7.25 (dd, $J = 7.8, 5.5$ Hz, 3H), 5.31 (s, 1H), 3.84 (d, $J =$
 858 11.3 Hz, 2H), 3.34 (d, $J = 6.9$ Hz, 2H), 3.30 – 3.24 (m, 2H), 2.64 (m, $J = 10.3, 5.1$ Hz,
 859 1H), 1.77 (d, $J = 11.4$ Hz, 2H), 1.31 (dd, $J = 19.3, 11.2$ Hz, 2H). ^{13}C NMR (101 MHz,
 860 DMSO- d_6) δ 163.95, 163.20, 148.91, 139.53, 137.01, 132.06, 122.77, 122.21, 122.06,
 861 121.82, 115.87, 114.59, 100.29, 59.98, 52.91, 52.56, 45.91, 25.00.

862 *2-(diethylamino)-N-(4-((2-oxo-1,2-dihydroquinolin-4-yl)oxy)phenyl)acetamide*

(16k). Yield: 55%; white solid; MS (ESI⁺): [M + H]⁺ calculated for C₂₁H₂₃N₃O₃, 365.1739; found, 366.1816; ¹H NMR (400 MHz, DMSO-*d*₆) δ 11.54 (s, 1H), 9.79 (s, 1H), 7.97 (d, *J* = 7.3 Hz, 1H), 7.80 (d, *J* = 8.9 Hz, 2H), 7.62 – 7.57 (m, 1H), 7.35 (d, *J* = 8.2 Hz, 1H), 7.29 – 7.19 (m, 3H), 5.31 (s, 1H), 3.18 (s, 2H), 2.62 (q, *J* = 7.1 Hz, 4H), 1.04 (t, *J* = 7.1 Hz, 6H). ¹³C NMR (101 MHz, DMSO-*d*₆) δ 170.37, 163.93, 163.19, 148.85, 139.53, 136.91, 132.03, 122.78, 122.17, 122.05, 121.57, 115.84, 114.61, 100.32, 57.81, 48.31, 40.65, 40.44, 40.23, 40.02, 39.82, 39.61, 39.40, 12.38.

2-(ethylamino)-N-(4-((2-oxo-1,2-dihydroquinolin-4-yl)oxy)phenyl)acetamide

(16l). Yield: 55%; white solid; MS (ESI⁺): [M + H]⁺ calculated for C₁₉H₁₉N₃O₃, 337.1426; found, 338.1505; ¹H NMR (400 MHz, DMSO-*d*₆) δ 11.56 (s, 1H), 10.45 (s, 1H), 7.97 (d, *J* = 7.3 Hz, 1H), 7.76 (d, *J* = 8.9 Hz, 2H), 7.68 – 7.55 (m, 1H), 7.36 (d, *J* = 8.2 Hz, 1H), 7.32 – 7.21 (m, 3H), 5.31 (s, 1H), 3.77 (s, 2H), 2.91 (q, *J* = 7.2 Hz, 2H), 1.18 (t, *J* = 7.2 Hz, 3H). ¹³C NMR (101 MHz, DMSO-*d*₆) δ 165.87, 163.87, 163.21, 149.18, 139.50, 136.55, 132.11, 122.77, 122.39, 122.26, 121.46, 115.87, 114.57, 100.33, 49.35, 42.86, 12.23.

N-(4-((2-oxo-1,2-dihydroquinolin-4-yl)oxy)phenyl)-2-(piperazin-1-yl)acetamide

(16m). Yield: 65%; white solid; MS (ESI⁺): [M + H]⁺ calculated for C₂₁H₂₂N₄O₃, 378.1692; found, 379.1721; ¹H NMR (400 MHz, DMSO-*d*₆) δ 11.58 (s, 1H), 9.91 (s, 1H), 7.97 (d, *J* = 7.8 Hz, 1H), 7.80 (d, *J* = 8.7 Hz, 2H), 7.60 (t, *J* = 7.5 Hz, 1H), 7.36 (d, *J* = 8.2 Hz, 1H), 7.25 (t, *J* = 6.9 Hz, 3H), 5.32 (s, 1H), 3.12 (s, 2H), 2.77 (s, 4H), 2.44 (s, 4H). ¹³C NMR (101 MHz, DMSO-*d*₆) δ 168.92, 163.94, 163.22, 148.82, 139.54, 137.07, 132.03, 122.78, 122.17, 122.03, 121.64, 115.87, 114.61, 100.31, 62.91, 54.37, 45.87.

885 *2-(4-ethylpiperazin-1-yl)-N-(4-((2-oxo-1,2-dihydroquinolin-4-yl)oxy)phenyl)-ace*
 886 *tamide (16n)*. Yield: 38%; white solid; MS (ESI⁺): [M + H]⁺ calculated for C₂₃H₂₆N₄O₃,
 887 406.2005; found, 407.2079; ¹H NMR (400 MHz, DMSO-*d*₆) δ 11.55 (s, 1H), 9.96 (s,
 888 1H), 7.97 (d, *J* = 7.8 Hz, 1H), 7.78 (d, *J* = 8.9 Hz, 2H), 7.61 (t, *J* = 7.7 Hz, 1H), 7.36 (d,
 889 *J* = 8.2 Hz, 1H), 7.26 (t, *J* = 7.9 Hz, 3H), 5.30 (s, 1H), 3.31 (s, 2H), 3.02 (m, 6H), 2.83 (q,
 890 4H), 1.20 (t, *J* = 7.1 Hz, 3H). ¹³C NMR (101 MHz, DMSO-*d*₆) δ 171.10, 163.95, 163.22,
 891 148.74, 139.52, 137.10, 132.05, 122.78, 122.20, 122.13, 121.31, 115.85, 114.61,
 892 100.27, 66.22, 53.83, 50.14, 33.51.

893 *2-(4-ethylpiperazin-1-yl)-N-(4-((2-oxo-1,2-dihydroquinolin-4-yl)oxy)phenyl)-ace*
 894 *tamide (16o)*. Yield: 53%; white solid; MS (ESI⁺): [M + H]⁺ calculated for C₂₃H₂₄N₄O₄,
 895 420.1798; found, 421.2087; ¹H NMR (400 MHz, DMSO-*d*₆) δ 11.54 (s, 1H), 9.92 (s,
 896 1H), 7.97 (d, *J* = 7.7 Hz, 1H), 7.79 (d, *J* = 8.9 Hz, 2H), 7.60 (t, *J* = 7.2 Hz, 1H), 7.35 (d,
 897 *J* = 8.2 Hz, 1H), 7.24 (dd, *J* = 7.9, 4.3 Hz, 3H), 5.31 (s, 1H), 3.51 (d, *J* = 4.1 Hz, 4H),
 898 3.20 (s, 2H), 2.57 – 2.53 (m, 2H), 2.48 (d, *J* = 4.8 Hz, 2H), 2.00 (s, 3H). ¹³C NMR (101
 899 MHz, DMSO-*d*₆) δ 168.39, 163.96, 163.22, 148.92, 139.50, 136.97, 132.09, 122.77,
 900 122.24, 122.11, 121.72, 115.86, 114.58, 100.28, 60.74, 51.38, 51.25, 50.20, 40.64,
 901 40.43, 40.22, 40.01, 39.80, 39.59, 39.38.

902 *4-(2-fluoro-4-nitrophenoxy)quinolin-2(1H)-one (17a)*. 4-hydroxy-2 (1H)
 903 -quinolinone (3.22 g, 0.02 mol) and K₂CO₃ (4.14 g, 0.03 mol) were dissolved in DMF
 904 (200 ml) and stir at room temperature. Subsequently, 3,4-difluoronitrobenzene (4.77 g,
 905 0.01 mol) was dissolved in another 20 ml of DMF and added dropwise to the previously
 906 stirred reaction solution within half an hour.. After the reaction was stirred overnight at

room temperature and then monitored by TLC the next day, 400 ml of pure water was added to it. Then solid was collected through a filter. After drying through a vacuum drying oven, a pale yellow solid was afforded as compound 13 (5.11 g, yield 85%). MS (ESI⁺): [M + H]⁺ calculated for C₁₅H₉FN₂O₄, 300.0546; found, 301.0623. ¹H NMR (400 MHz, DMSO-*d*₆) δ 11.76 (s, 1H), 8.45 (dd, *J* = 10.4, 2.7 Hz, 1H), 8.22 (ddd, *J* = 9.0, 2.6, 1.3 Hz, 1H), 7.93 (dd, *J* = 8.0, 1.0 Hz, 1H), 7.81 – 7.72 (m, 1H), 7.68 – 7.58 (m, 1H), 7.40 (d, *J* = 8.2 Hz, 1H), 7.32 – 7.23 (m, 1H), 5.68 (s, 1H).

6-(2-fluoro-4-nitrophenoxy)quinolin-2(1H)-one (17b). Compound 17b was prepared as the same method as compound 17a; brown solid, yield 82%. MS (ESI⁺): [M + H]⁺ calculated for C₁₅H₉FN₂O₄, 300.0546; found, 301.0623. ¹H NMR (400 MHz, DMSO-*d*₆) δ 11.91 (s, 1H), 8.34 (dd, *J* = 10.8, 2.7 Hz, 1H), 8.09 – 8.02 (m, 1H), 7.88 (d, *J* = 9.6 Hz, 1H), 7.56 (d, *J* = 1.2 Hz, 1H), 7.43 (d, *J* = 2.3 Hz, 2H), 7.13 (t, *J* = 8.7 Hz, 1H), 6.56 (d, *J* = 9.6 Hz, 1H).

7-(2-fluoro-4-nitrophenoxy)quinolin-2(1H)-one (17c). Compound 17c was prepared as the same method as compound 17a; brown solid, yield 86%. MS (ESI⁺): [M + H]⁺ calculated for C₁₅H₉FN₂O₄, 300.0546; found, 301.0623. ¹H NMR (400 MHz, DMSO-*d*₆) δ 11.73 (s, 1H), 8.40 (dd, *J* = 10.7, 2.7 Hz, 1H), 8.13 (ddd, *J* = 9.1, 2.6, 1.3 Hz, 1H), 7.92 (d, *J* = 9.6 Hz, 1H), 7.76 (d, *J* = 8.5 Hz, 1H), 7.39 (t, *J* = 8.6 Hz, 1H), 7.04 – 6.97 (m, 2H), 6.46 (d, *J* = 9.5 Hz, 1H).

4-(4-amino-2-fluorophenoxy)quinolin-2(1H)-one (18a). Compound 18a was prepared as the same method as compound 14; brown solid, yield 90%. MS (ESI⁺): [M + H]⁺ calculated for C₁₅H₁₁FN₂O₂, 270.0805; found, 271.0883. ¹H NMR (400 MHz,

929 DMSO-*d*₆) δ 11.60 (s, 1H), 7.95 (d, *J* = 7.7 Hz, 1H), 7.60 (t, *J* = 7.4 Hz, 1H), 7.36 (q, *J*
930 = 8.8 Hz, 5H), 7.25 (t, *J* = 7.3 Hz, 1H), 5.33 (s, 1H).

931 *6-(4-amino-2-fluorophenoxy)quinolin-2(1H)-one (18b)*. Compound 18b was
932 prepared as the same method as compound 14; brown solid, yield 90%. MS (ESI⁺): [M
933 + H]⁺ calculated for C₁₅H₁₁FN₂O₂, 270.0805; found, 271.0883. ¹H NMR (400 MHz,
934 DMSO-*d*₆) δ 11.87 (s, 1H), 7.88 (d, *J* = 9.5 Hz, 1H), 7.45 – 7.35 (m, 2H), 7.31 (d, *J* =
935 6.8 Hz, 2H), 7.25 – 7.12 (m, 2H), 6.52 (d, *J* = 9.4 Hz, 1H).

936 *7-(4-amino-2-fluorophenoxy)quinolin-2(1H)-one (18c)*. Compound 18c was
937 prepared as the same method as compound 14; brown solid, yield 90%. MS (ESI⁺): [M
938 + H]⁺ calculated for C₁₅H₁₁FN₂O₂, 270.0805; found, 271.0883. ¹H NMR (400 MHz,
939 DMSO-*d*₆) δ 11.59 (s, 1H), 7.86 (d, *J* = 9.5 Hz, 1H), 7.67 (d, *J* = 8.5 Hz, 1H), 7.33 (dd,
940 *J* = 15.3, 8.0 Hz, 2H), 7.14 (d, *J* = 7.4 Hz, 1H), 6.91 – 6.77 (m, 2H), 6.38 (d, *J* = 9.4 Hz,
941 1H).

942 *2-chloro-N-(3-fluoro-4-((2-oxo-1,2-dihydroquinolin-4-yl)oxy)phenyl)acetamide*
943 *(19a)*. Compound 19a was prepared as the same method as compound 15; brown solid,
944 yield 95%. MS (ESI⁺): [M + H]⁺ calculated for C₁₇H₁₂FN₂O₃Cl, 346.0520; found,
945 347.0599. ¹H NMR (400 MHz, DMSO-*d*₆) δ 11.63 (s, 1H), 10.69 (s, 1H), 7.92 (dd, *J* =
946 56.5, 9.6 Hz, 2H), 7.62 (s, 1H), 7.47 (s, 2H), 7.37 (d, *J* = 7.3 Hz, 1H), 7.27 (s, 1H), 5.35
947 (s, 1H), 4.31 (s, 2H).

948 *2-chloro-N-(3-fluoro-4-((2-oxo-1,2-dihydroquinolin-6-yl)oxy)phenyl)acetamide*
949 *(19b)*. Compound 19b was prepared as the same method as compound 15; brown solid,
950 yield 95%. MS (ESI⁺): [M + H]⁺ calculated for C₁₇H₁₂FN₂O₃Cl, 346.0520; found,

347.0599. ^1H NMR (400 MHz, DMSO- d_6) δ 11.80 (s, 1H), 11.31 (s, 1H), 7.83 (dd, J = 17.0, 5.7 Hz, 2H), 7.46 (d, J = 8.7 Hz, 1H), 7.37 (d, J = 8.9 Hz, 1H), 7.25 (dd, J = 8.9, 2.5 Hz, 1H), 7.18 (dd, J = 15.0, 5.7 Hz, 2H), 6.48 (d, J = 9.5 Hz, 1H), 4.36 (s, 2H).

2-chloro-N-(3-fluoro-4-((2-oxo-1,2-dihydroquinolin-7-yl)oxy)phenyl)acetamide (19c). Compound 19c was prepared as the same method as compound 15; brown solid, yield 95%. MS (ESI $^+$): $[\text{M} + \text{H}]^+$ calculated for $\text{C}_{17}\text{H}_{12}\text{FN}_2\text{O}_3\text{Cl}$, 346.0520; found, 347.0599. ^1H NMR (400 MHz, DMSO- d_6) δ 11.50 (s, 1H), 11.01 (s, 1H), 7.84 (s, 2H), 7.64 (d, J = 8.3 Hz, 1H), 7.45 (s, 1H), 7.33 (d, J = 8.3 Hz, 1H), 6.80 (dd, J = 40.5, 13.0 Hz, 2H), 6.36 (d, J = 8.9 Hz, 1H), 4.34 (s, 2H).

General procedure for synthesis of compounds 20a-20o, 21a-21c and 22a-22c was same as compounds 16a-16o.

N-(3-fluoro-4-((2-oxo-1,2-dihydroquinolin-4-yl)oxy)phenyl)-2-(pyrrolidin-1-yl)acetamide (20a). Yield: 72%; white solid; MS (ESI $^+$): $[\text{M} + \text{H}]^+$ calculated for $\text{C}_{21}\text{H}_{20}\text{FN}_3\text{O}_3$, 381.1489; found, 382.1565; ^1H NMR (400 MHz, DMSO- d_6) δ 11.70 (s, 1H), 10.53 (s, 1H), 7.96 (dd, J = 19.8, 5.3 Hz, 2H), 7.62 (d, J = 7.1 Hz, 2H), 7.43 (t, J = 8.7 Hz, 2H), 7.27 (s, 1H), 5.34 (s, 1H), 3.44 (s, 2H), 2.70 (s, 4H), 1.78 (s, 4H).

N-(3-fluoro-4-((2-oxo-1,2-dihydroquinolin-4-yl)oxy)phenyl)-2-(piperidin-1-yl)acetamide (20b). Yield: 86%; white solid; MS (ESI $^+$): $[\text{M} + \text{H}]^+$ calculated for $\text{C}_{22}\text{H}_{22}\text{FN}_3\text{O}_3$, 395.1645; found, 396.1721; ^1H NMR (400 MHz, DMSO- d_6) δ 11.61 (s, 1H), 10.26 (s, 1H), 7.97 (dd, J = 9.0, 6.3 Hz, 2H), 7.62 (dd, J = 12.0, 4.8 Hz, 2H), 7.41 (q, J = 8.9 Hz, 2H), 7.27 (t, J = 8.0 Hz, 1H), 5.34 (s, 1H), 3.13 (s, 2H), 2.49 – 2.42 (m, 4H), 1.61 – 1.52 (m, 4H), 1.40 (d, J = 4.8 Hz, 2H). ^{13}C NMR (101 MHz, DMSO- d_6) δ

163.03, 162.99, 154.75, 152.30, 139.50, 138.50, 138.40, 135.39, 135.27, 132.20,
124.49, 122.70, 122.36, 116.71, 115.98, 114.03, 108.70, 108.47, 99.71, 54.13, 24.90,
23.30.

N-(3-fluoro-4-((2-oxo-1,2-dihydroquinolin-4-yl)oxy)phenyl)-2-morpholino-acetamide (20c). Yield: 82%; white solid; MS (ESI⁺): [M + H]⁺ calculated for C₂₁H₂₀FN₃O₄, 397.1438; found, 398.1525; ¹H NMR (400 MHz, DMSO-*d*₆) δ 11.67 (s, 1H), 10.31 (s, 1H), 7.97 (ddd, *J* = 15.4, 10.6, 1.6 Hz, 2H), 7.66 – 7.55 (m, 2H), 7.42 (dd, *J* = 18.4, 9.1 Hz, 2H), 7.31 – 7.21 (m, 1H), 5.34 (s, 1H), 3.70 – 3.58 (m, 4H), 3.20 (s, 2H), 2.57 – 2.52 (m, 4H). ¹³C NMR (101 MHz, DMSO-*d*₆) δ 169.17, 163.08, 163.04, 154.72, 152.28, 139.47, 138.68, 138.58, 135.24, 135.12, 132.20, 124.39, 122.70, 122.37, 116.73, 115.98, 114.04, 108.73, 108.50, 99.66, 66.53, 62.34, 53.58.

N-(3-fluoro-4-((2-oxo-1,2-dihydroquinolin-4-yl)oxy)phenyl)-2-(4-methyl-piperidin-1-yl)acetamide (20d). Yield: 81%; white solid; MS (ESI⁺): [M + H]⁺ calculated for C₂₃H₂₄FN₃O₃, 409.1802; found, 410.1879; ¹H NMR (400 MHz, DMSO-*d*₆) δ 11.66 (s, 1H), 10.36 (s, 1H), 8.04 – 7.89 (m, 2H), 7.61 (dd, *J* = 14.2, 7.3 Hz, 2H), 7.42 (dd, *J* = 20.1, 8.7 Hz, 2H), 7.27 (t, *J* = 7.6 Hz, 1H), 5.34 (s, 1H), 3.17 (d, *J* = 4.2 Hz, 2H), 2.92 (s, 2H), 2.26 (s, 2H), 1.61 (d, *J* = 11.8 Hz, 2H), 1.30 (dd, *J* = 21.9, 10.5 Hz, 3H), 0.92 (d, *J* = 6.0 Hz, 3H). ¹³C NMR (101 MHz, DMSO-*d*₆) δ 163.04, 163.01, 154.74, 152.30, 139.50, 138.61, 138.51, 135.28, 135.16, 132.19, 124.42, 122.70, 122.34, 116.68, 115.97, 114.04, 108.68, 108.46, 99.70, 53.73, 33.75, 30.04, 22.14.

N-(3-fluoro-4-((2-oxo-1,2-dihydroquinolin-4-yl)oxy)phenyl)-2-(4-methyl-piperazin-1-yl)acetamide (20e). Yield: 48%; white solid; MS (ESI⁺): [M + H]⁺ calculated for

995 $C_{22}H_{23}FN_4O_3$, 410.1754; found, 411.1821; 1H NMR (400 MHz, DMSO- d_6) δ 11.67 (s,
996 1H), 10.28 (s, 1H), 7.96 (dd, $J = 19.0, 10.6$ Hz, 2H), 7.60 (dd, $J = 16.8, 8.6$ Hz, 2H),
997 7.42 (dd, $J = 16.5, 8.4$ Hz, 2H), 7.27 (t, $J = 7.5$ Hz, 1H), 5.34 (s, 1H), 3.19 (s, 2H), 2.55
998 (s, 4H), 2.44 (s, 4H), 2.21 (s, 3H). ^{13}C NMR (101 MHz, DMSO- d_6) δ 169.30, 163.04,
999 154.73, 152.29, 139.50, 138.72, 138.62, 135.21, 135.08, 132.18, 124.39, 122.70,
1000 122.33, 116.66, 115.97, 114.04, 108.65, 108.42, 99.69, 62.01, 54.81, 52.86, 45.96.

1001 *2-(4-(cyclopropanecarbonyl)piperazin-1-yl)-N-(3-fluoro-4-((2-oxo-1,2-dihydro-q*
1002 *uinolin-4-yl)oxy)phenyl)acetamide (20f)*. Yield: 90%; white solid; MS (ESI⁺): [M + H]⁺
1003 calculated for $C_{25}H_{25}FN_4O_4$, 464.1860; found, 465.1940; 1H NMR (400 MHz,
1004 DMSO- d_6) δ 11.70 (s, 1H), 10.53 (s, 1H), 8.02 – 7.94 (m, 2H), 7.62 (t, $J = 8.0$ Hz, 2H),
1005 7.44 (t, $J = 8.7$ Hz, 2H), 7.27 (t, $J = 7.4$ Hz, 1H), 5.34 (s, 1H), 3.74 (s, 2H), 3.53 (s, 2H),
1006 3.27 (s, 2H), 2.59 (s, 2H), 1.98 (s, 1H), 0.71 (m, 4H). ^{13}C NMR (101 MHz, DMSO- d_6)
1007 δ 171.48, 163.02, 162.77, 154.77, 152.33, 139.49, 138.50, 138.40, 135.37, 135.25,
1008 132.22, 124.47, 122.72, 122.35, 116.76, 115.92, 114.05, 108.81, 108.58, 99.72, 61.68,
1009 45.07, 41.82, 10.69, 7.44.

1010 *2-(4-acetylpiperazin-1-yl)-N-(3-fluoro-4-((2-oxo-1,2-dihydroquinolin-4-yl)oxy)-p*
1011 *henyl)acetamide (20g)*. Yield: 88%; white solid; MS (ESI⁺): [M + H]⁺ calculated for
1012 $C_{25}H_{25}FN_4O_4$, 438.1703; found, 439.1784; 1H NMR (400 MHz, DMSO- d_6) δ 11.69 (s,
1013 1H), 10.46 (s, 1H), 7.97 (t, $J = 10.6$ Hz, 2H), 7.62 (s, 2H), 7.47 – 7.39 (m, 2H), 7.27 (t,
1014 $J = 7.5$ Hz, 1H), 5.34 (s, 1H), 3.50 (d, $J = 3.8$ Hz, 4H), 3.26 (s, 2H), 2.56 (s, 2H), 2.50 –
1015 2.46 (m, 2H), 2.00 (s, 3H). ^{13}C NMR (101 MHz, DMSO- d_6) δ 169.20, 168.63, 163.04,
1016 154.72, 152.28, 139.50, 138.72, 138.62, 135.24, 135.11, 132.19, 124.39, 122.70,

122.34, 116.70, 115.97, 114.04, 108.71, 108.49, 99.69, 61.73, 53.24, 46.05, 21.64.

2-(4-(dimethylamino)piperidin-1-yl)-N-(3-fluoro-4-((2-oxo-1,2-dihydroquinolin-4-yl)oxy)phenyl)acetamide (20h). Yield: 48%; white solid; MS (ESI⁺): [M + H]⁺ calculated for C₂₄H₂₇FN₄O₃, 438.2067; found, 439.2140; ¹H NMR (400 MHz, DMSO-*d*₆) δ 11.67 (s, 1H), 10.39 (s, 1H), 8.02 – 7.92 (m, 2H), 7.66 – 7.57 (m, 2H), 7.43 (dd, *J* = 17.8, 8.7 Hz, 2H), 7.27 (dd, *J* = 11.2, 4.1 Hz, 1H), 5.34 (s, 1H), 3.24 (s, 2H), 3.00 (s, 3H), 2.66 (s, 6H), 2.24 (t, *J* = 11.4 Hz, 2H), 2.00 (d, *J* = 10.9 Hz, 2H), 1.77 (dd, *J* = 11.9, 3.2 Hz, 2H). ¹³C NMR (101 MHz, DMSO-*d*₆) δ 169.33, 163.05, 154.72, 152.27, 139.49, 138.73, 138.63, 135.22, 135.09, 132.21, 124.39, 122.70, 122.37, 116.70, 115.98, 114.03, 108.71, 108.48, 99.67, 62.43, 61.30, 51.83, 39.49, 26.01.

tert-butyl 4-(2-((3-fluoro-4-((2-oxo-1,2-dihydroquinolin-4-yl)oxy)phenyl)amino)-2-oxoethyl)piperazine-1-carboxylate (20i). Yield: 85%; white solid; MS (ESI⁺): [M + H]⁺ calculated for C₂₆H₂₉FN₄O₅, 496.2122; found, 497.2205; ¹H NMR (400 MHz, DMSO-*d*₆) δ 11.63 (s, 1H), 10.08 (s, 1H), 7.95 (dd, *J* = 30.0, 10.2 Hz, 2H), 7.58 (dd, *J* = 20.2, 7.5 Hz, 2H), 7.49 – 7.19 (m, 3H), 5.34 (s, 1H), 3.40 (s, 4H), 3.20 (s, 2H), 2.50 (s, 4H), 1.41 (s, 9H). ¹³C NMR (101 MHz, DMSO-*d*₆) δ 169.13, 163.01, 154.77, 154.34, 152.33, 139.49, 138.43, 135.33, 132.22, 124.44, 122.73, 122.33, 116.74, 115.92, 114.05, 108.79, 108.58, 99.72, 79.27, 61.98, 52.89, 43.72, 28.53.

2-(4-(tert-butyl)piperazin-1-yl)-N-(3-fluoro-4-((2-oxo-1,2-dihydroquinolin-4-yl)oxy)phenyl)acetamide (20j). Yield: 79%; white solid; MS (ESI⁺): [M + H]⁺ calculated for C₂₅H₂₉FN₄O₃, 452.2224; found, 453.2300; ¹H NMR (400 MHz, DMSO-*d*₆) δ 11.69 (s, 1H), 10.33 (s, 1H), 7.95 (dd, *J* = 19.0, 5.3 Hz, 2H), 7.61 (t, *J* = 7.3 Hz, 2H), 7.45 –

7.38 (m, 2H), 7.26 (t, $J = 7.5$ Hz, 1H), 5.33 (s, 1H), 3.15 (s, 2H), 2.52-2.42 (, 8H), 1.01 (s, 9H). ^{13}C NMR (101 MHz, DMSO- d_6) δ 169.35, 163.03, 154.72, 152.29, 139.51, 138.72, 135.08, 132.19, 124.38, 122.70, 122.34, 116.71, 115.98, 114.04, 108.69, 99.69, 62.17, 53.98, 45.56, 36.27, 26.09.

2-(diethylamino)-N-(3-fluoro-4-((2-oxo-1,2-dihydroquinolin-4-yl)oxy)phenyl)-acetamide (20k). Yield: 75%; white solid; MS (ESI $^+$): $[\text{M} + \text{H}]^+$ calculated for $\text{C}_{21}\text{H}_{22}\text{FN}_3\text{O}_3$, 383.1645; found, 384.1722; ^1H NMR (400 MHz, DMSO- d_6) δ 11.67 (s, 1H), 10.32 (s, 1H), 7.97 (ddd, $J = 15.5, 10.6, 1.6$ Hz, 2H), 7.67 – 7.58 (m, 2H), 7.48 – 7.37 (m, 2H), 7.27 (dd, $J = 11.3, 4.0$ Hz, 1H), 5.35 (s, 1H), 2.70 (d, $J = 5.8$ Hz, 4H), 1.06 (t, $J = 7.1$ Hz, 6H). ^{13}C NMR (101 MHz, DMSO- d_6) δ 163.03, 163.01, 154.76, 152.32, 139.51, 138.49, 138.39, 135.32, 135.20, 132.18, 124.43, 122.70, 122.33, 116.68, 115.97, 114.04, 108.68, 108.45, 99.72, 57.01, 48.27, 11.99.

2-(ethylamino)-N-(3-fluoro-4-((2-oxo-1,2-dihydroquinolin-4-yl)oxy)phenyl)acetamide (20l). Yield: 62%; white solid; MS (ESI $^+$): $[\text{M} + \text{H}]^+$ calculated for $\text{C}_{19}\text{H}_{18}\text{FN}_3\text{O}_3$, 355.1332; found, 356.1407; ^1H NMR (400 MHz, DMSO- d_6) δ 11.63 (s, 1H), 7.99 (d, $J = 7.3$ Hz, 1H), 7.92 (dd, $J = 13.1, 2.3$ Hz, 1H), 7.66 – 7.59 (m, 1H), 7.54 (dd, $J = 8.9, 1.4$ Hz, 1H), 7.44 (t, $J = 8.9$ Hz, 1H), 7.37 (d, $J = 8.2$ Hz, 1H), 7.27 (t, $J = 7.4$ Hz, 1H), 5.34 (s, 1H), 3.33 (s, 3H), 2.60 (q, $J = 7.1$ Hz, 2H), 1.06 (t, $J = 7.1$ Hz, 3H).

N-(3-fluoro-4-((2-oxo-1,2-dihydroquinolin-4-yl)oxy)phenyl)-2-(piperazin-1-yl)acetamide (20m). Yield: 95%; white solid; MS (ESI $^+$): $[\text{M} + \text{H}]^+$ calculated for $\text{C}_{21}\text{H}_{21}\text{FN}_4\text{O}_3$, 396.1598; found, 397.1874; ^1H NMR (400 MHz, DMSO- d_6) δ 10.04 (s, 1H), 7.98 (d, $J = 8.0$ Hz, 1H), 7.91 (d, $J = 13.0$ Hz, 1H), 7.65 – 7.51 (m, 2H), 7.47 – 7.33

(m, 2H), 7.26 (t, $J = 7.6$ Hz, 1H), 5.34 (s, 1H), 3.13 (s, 2H), 2.79 (s, 4H), 2.46 (s, 4H).

N-(3-fluoro-4-((2-oxo-1,2-dihydroquinolin-4-yl)oxy)phenyl)-2-((tetrahydro-2H-pyran-4-yl)amino)acetamide (20n). Yield: 64%; white solid; MS (ESI⁺): [M + H]⁺ calculated for C₂₁H₂₁FN₄O₃, 411.1594; found, 412.1878; ¹H NMR (400 MHz, DMSO-*d*₆) δ 11.63 (s, 1H), 10.16 (s, 1H), 7.99 (dd, $J = 8.0, 1.0$ Hz, 1H), 7.93 (dd, $J = 13.1, 2.3$ Hz, 1H), 7.65 – 7.59 (m, 1H), 7.54 (dd, $J = 8.9, 1.4$ Hz, 1H), 7.44 (t, $J = 8.9$ Hz, 1H), 7.37 (d, $J = 8.1$ Hz, 1H), 7.27 (dd, $J = 11.6, 4.5$ Hz, 1H), 5.34 (s, 1H), 3.84 (dt, $J = 11.4, 3.4$ Hz, 2H), 3.33 (s, 2H), 3.28 (dd, $J = 11.5, 2.0$ Hz, 3H), 2.64 (ddd, $J = 14.3, 10.2, 4.0$ Hz, 1H), 1.77 (dd, $J = 12.5, 1.7$ Hz, 2H), 1.35 – 1.25 (m, 2H).

2-(4-ethylpiperazin-1-yl)-*N*-(3-fluoro-4-((2-oxo-1,2-dihydroquinolin-4-yl)oxy)phenyl)acetamide (20o). Yield: 53%; white solid; MS (ESI⁺): [M + H]⁺ calculated for C₂₁H₂₁FN₄O₃, 424.1911; found, 425.1987; ¹H NMR (400 MHz, DMSO-*d*₆) δ 11.70 (s, 1H), 10.42 (s, 1H), 8.02 – 7.92 (m, 2H), 7.66 – 7.57 (m, 2H), 7.43 (t, $J = 9.0$ Hz, 2H), 7.30 – 7.23 (m, 1H), 5.34 (s, 1H), 3.36 (s, 4H), 3.23 (s, 2H), 2.63 (m, 6H), 1.06 (m, 3H). ¹³C NMR (101 MHz, DMSO-*d*₆) δ 169.21, 163.05, 154.72, 152.28, 139.50, 138.71, 138.61, 135.22, 135.10, 132.19, 124.39, 122.70, 122.35, 116.66, 115.98, 114.04, 108.68, 108.45, 99.68, 61.74, 52.23, 52.04, 51.76, 11.58.

2-(4-(cyclopropanecarbonyl)piperazin-1-yl)-*N*-(3-fluoro-4-((2-oxo-1,2-dihydroquinolin-6-yl)oxy)phenyl)acetamide (21a). Yield: 90%; white solid; MS (ESI⁺): [M + H]⁺ calculated for C₂₅H₂₅FN₄O₄, 464.1860; found, 465.1941; ¹H NMR (400 MHz, DMSO-*d*₆) δ 11.73 (s, 1H), 9.99 (s, 1H), 7.88 – 7.79 (m, 2H), 7.43 (d, $J = 8.9$ Hz, 1H), 7.32 (d, $J = 8.9$ Hz, 1H), 7.26 (dd, $J = 8.9, 2.6$ Hz, 1H), 7.22 – 7.13 (m, 2H), 6.50 (d, $J =$

9.6 Hz, 1H), 3.74 (s, 2H), 3.54 (s, 2H), 3.20 (s, 2H), 2.56 (s, 2H), 2.50 (s, 2H), 1.97 (m, $J = 12.6, 7.7, 4.8$ Hz, 1H), 0.77 – 0.69 (m, 4H).

tert-butyl 4-(2-((3-fluoro-4-((2-oxo-1,2-dihydroquinolin-6-yl)oxy)phenyl)amino)-2-oxoethyl)piperazine-1-carboxylate (21b). Yield: 78%; white solid; MS (ESI⁺): [M + H]⁺ calculated for C₂₆H₂₉FN₄O₅, 496.2122; found, 497.2261; ¹H NMR (400 MHz, DMSO-*d*₆) δ 11.73 (s, 1H), 9.98 (s, 1H), 7.83 (t, $J = 10.4$ Hz, 2H), 7.42 (d, $J = 8.6$ Hz, 1H), 7.35 – 7.22 (m, 2H), 7.17 (dd, $J = 17.8, 8.7$ Hz, 2H), 6.49 (d, $J = 9.5$ Hz, 1H), 3.38 (s, 4H), 3.17 (s, 2H), 2.48 (d, $J = 4.9$ Hz, 4H), 1.40 (s, 9H).

2-(4-(tert-butyl)piperazin-1-yl)-N-(3-fluoro-4-((2-oxo-1,2-dihydroquinolin-6-yl)oxy)phenyl)acetamide (21c). Yield: 65%; white solid; MS (ESI⁺): [M + H]⁺ calculated for C₂₅H₂₉FN₄O₃, 452.2224; found, 453.2299; ¹H NMR (400 MHz, DMSO-*d*₆) δ 11.73 (s, 1H), 10.00 (s, 1H), 7.82 (t, $J = 12.0$ Hz, 2H), 7.47 – 7.08 (m, 5H), 6.50 (d, $J = 9.6$ Hz, 1H), 3.48 (s, 2H), 3.32 (s, 2H), 3.09 (s, 4H), 2.70 (s, 2H), 1.34 (s, 9H).

2-(4-(cyclopropanecarbonyl)piperazin-1-yl)-N-(3-fluoro-4-((2-oxo-1,2-dihydroquinolin-7-yl)oxy)phenyl)acetamide (22a). Yield: 92%; white solid; MS (ESI⁺): [M + H]⁺ calculated for C₂₅H₂₅FN₄O₄, 464.1860; found, 465.1940; ¹H NMR (400 MHz, DMSO-*d*₆) δ 11.48 (s, 1H), 10.06 (s, 1H), 7.91 – 7.81 (m, 2H), 7.64 (d, $J = 8.7$ Hz, 1H), 7.50 (d, $J = 8.8$ Hz, 1H), 7.30 (t, $J = 9.0$ Hz, 1H), 6.84 (dd, $J = 8.6, 2.3$ Hz, 1H), 6.76 (d, $J = 2.1$ Hz, 1H), 6.36 (d, $J = 9.5$ Hz, 1H), 3.74 (s, 2H), 3.54 (s, 2H), 3.21 (s, 2H), 2.57 (s, 2H), 2.50 – 2.45 (m, 2H), 2.03 – 1.91 (m, 1H), 0.78 – 0.64 (m, 4H).

tert-butyl 4-(2-((3-fluoro-4-((2-oxo-1,2-dihydroquinolin-7-yl)oxy)phenyl)amino)-2-oxoethyl)piperazine-1-carboxylate (22b). Yield: 86%; white solid; MS (ESI⁺): [M +

$\text{H}]^+$ calculated for $\text{C}_{26}\text{H}_{29}\text{FN}_4\text{O}_5$, 496.2122; found, 497.2205; ^1H NMR (400 MHz, $\text{DMSO}-d_6$) δ 11.48 (s, 1H), 10.03 (s, 1H), 7.86 (dd, $J = 11.5, 5.6$ Hz, 2H), 7.64 (d, $J = 8.6$ Hz, 1H), 7.49 (d, $J = 8.9$ Hz, 1H), 7.30 (t, $J = 9.0$ Hz, 1H), 6.84 (dd, $J = 8.6, 2.1$ Hz, 1H), 6.76 (s, 1H), 6.36 (d, $J = 9.5$ Hz, 1H), 3.37 (d, $J = 13.9$ Hz, 4H), 3.19 (s, 2H), 2.48 (s, 3H), 1.40 (s, 9H).

2-(4-(tert-butyl)piperazin-1-yl)-N-(3-fluoro-4-((2-oxo-1,2-dihydroquinolin-7-yl)oxy)phenyl)acetamide (22c). Yield: 75%; white solid; MS (ESI^+): $[\text{M} + \text{H}]^+$ calculated for $\text{C}_{25}\text{H}_{29}\text{FN}_4\text{O}_3$, 452.2224; found, 453.2300; ^1H NMR (400 MHz, $\text{DMSO}-d_6$) δ 11.50 (s, 1H), 10.05 (s, 1H), 7.89 – 7.80 (m, 2H), 7.65 (d, $J = 8.7$ Hz, 1H), 7.48 (d, $J = 8.8$ Hz, 1H), 7.31 (t, $J = 9.0$ Hz, 1H), 6.83 (dd, $J = 8.6, 2.4$ Hz, 1H), 6.77 (d, $J = 2.1$ Hz, 1H), 6.36 (d, $J = 9.5$ Hz, 1H), 3.59 – 3.39 (m, 2H), 3.32 (s, 2H), 3.11 (d, $J = 39.2$ Hz, 4H), 2.70 (s, 2H), 1.32 (s, 9H).

5.2 Biology

Cell culture

Rat kidney interstitial fibroblasts (NRK-49F cell line) were cultured in Dulbecco's Modified Eagle's Medium (DMEM) medium supplemented with 10% fetal bovine serum (FBS) and antibiotics (100 $\mu\text{g}/\text{ml}$ streptomycin, and 100 U/ml penicillin G) in a 37°C atmosphere of 95% humidified air and 5% CO_2 .

Mouse fibroblast L929 were cultured in minimum Eagle's medium (MEM) medium supplemented with 10% fetal bovine serum (FBS) and antibiotics (100 $\mu\text{g}/\text{ml}$ streptomycin, and 100 U/ml penicillin G) in a 37°C atmosphere of 95% humidified air

and 5% CO₂.

Collagen accumulation inhibition rate *in vitro*.

The anti-fibrosis activities of the compounds were tested in NRK-49F cells. NRK-49F cells were subcultured in DMEM medium containing penicillin 10% FBS, 50 U/ml penicillin and streptomycin in 50 ug/ml, and incubated in 5% CO₂ and 37°C incubators. Then the NRK-49F cells were covered with 96 orifice plates (1 x 10⁴ cells/hole), cultured with DMEM plus 5% FBS medium for three days. Then the supernatant was removed and DMEM plus 1% ITS was added for other two days. Next the supernatant was removed and the DMEM plus 1% ITS medium containing TGF-β (5 ng/ml) with or without 10 μM tested compounds to be tested was cultured for two days. Then removed the supernatant and added 4% paraformaldehyde (100 μl/hole) and fixed cells for thirty minutes at room temperature. Next cells were washed with PBS twice and 0.1% PSR dye solution (100 μl/hole) was added into cells, which were then incubated at room temperature for 4 h. Then removed of the dyeing liquid, added 0.1% acetic acid (100 μl/ hole) three times to clean excess dye, dried and photographed cells under a microscope camera. Last, added 0.1 M NaOH (100 μl/ hole), shaken and dissolved at room temperature for thirty minutes. Determine of each hole OD under wavelength 540 nm to test which compound could inhibit collagen deposition. Total collagen accumulation inhibition = (Administration A value - control A value) / (model A value - control A value) ×100%. All assays were repeated in triplicate.

Cell Survival Rate Measured by MTT Assay.

The NRK-49F cells were plated in a 96-well plate at a density of 0.5×10^5 cells/ml in a 100 μ l suspension and cultured overnight and the experimental group were added drugs at the concentration of 10 μ M. After 72 h, 20 μ l of 5% (m/v) MTT solution was added to each well and incubated for 4 hours in the incubator. Then each well was added 150 μ l DMSO-*d6*. Finally, the absorbance (A value) of each well was measured on a microplate reader. Survival rate=Administration A value - Zero A value / (Blank A value - Zero A value) $\times 100\%$. All assays were repeated in triplicate.

Inhibition of L929 Cells Migration Assay

L929 cells were grown on a 35 mm dish to 100% confluence and then scratched to form a 100 μ m wound using sterile pipette tips. The cells were then cultured in the presence or absence of TGF- β (5 ng/ml) and compounds (10 μ M) in serum-free media for 24 h. Images of the cells were taken at 0, 12 and 24 h using a light microscope (Nikon, Japan).

Western Blot Analysis.

The protein lysates were harvested using RIPA buffer with 1 mM phenylmethanesulfonyl fluoride (PMSF) and protease inhibitor cocktail, the protein concentration was determined by a bicinchoninic acid (BCA) kit. Same Proteins (30–40 μ g) of each sample were separated on 10%-12% SDS/PAGE gels at 80 V for 20 minutes and then turn to 120 V for 1 h. And proteins were transferred onto PVDF membranes at 80-100 V for 1.5 h, membranes were blocked in 5% (wt/vol) dried milk in PBS with 1‰ Tween 20 and then incubated with the indicated primary antibodies at 4°C overnight. After incubation with HRP-conjugated secondary antibodies,

immunoreactive bands were detected with the SuperLumia ECL Plus HRP Substrate Kit Solution (K22030, ABBKine). Primary antibodies used were: α -SMA (251411, ZENBIO), collagen I (14695-1-AP, Proteintech), p-smad3 (AF3363, Affinity), p-smad2 (18338S, CST), Smad2 (5339S, CST), Smad3 (9523S, CST), p-p38 (ab4822, abcam), p38 (ab170099, abcam), ERK1/2 (ab17942, abcam), p-ERK1/2 (340767, ZENBIO), β -actin (AB2001, Abways), GAPDH (AB0037, Abways), secondary antibodies used were: Goat Anti-Rabbit IgG (H+L) HRP (AB0101, Abways), Goat Anti-Mouse IgG (H+L) HRP (AB0102, Abways).

Bleomycin-Induced Lung Fibrosis Model.

Male C57BL/6 mice were obtained from Chengdu Dossy Experimental Animals CO, LTD, and 8-week-old mice were used in all experiments. C57BL/6 mice were randomly divided into eight groups (n=10 each group). Lung fibrosis was induced in male C57BL/6 mice by a single intratracheal instillation of 3 U/kg of bleomycin in 0.075 mL of saline, and control mice received an equal volume of saline only. There are six groups of drug treatments: mice were orally administered daily with nintedanib (50 mg/kg), **20f** (50 mg/kg) and **20f** (100 mg/kg) from day 1 to day 30 (prevention model) or day 8 to day 21 (treatment model).

Hydroxyproline Assay

The collagen contents in right lungs of mice were measured with a conventional Hydroxyproline assay kit (Nanjing Jiancheng Bioengineering Institute, A030-2). In a word, the right lungs were dried and acid hydrolyzed, then the residue was filtered

and the pH value was adjusted to 6.5-8.0. The hydroxyproline analysis was performed using chloramine-T spectrophotometric absorbance.

Hematoxylin-Eosin Staining (H&E staining), Masson Staining and Immunohistochemistry Staining

Left lungs were fixed in 10% formalin for 24 h and embedded in paraffin. Then lung sections (5 μ m) were prepared and stained with hematoxylin-eosin staining and Masson's trichrome staining, and also incubated with the antibody at 4 $^{\circ}$ C overnight for immunohistochemistry staining. Images were collected using an upright transmission fluorescence microscope.

Abbreviations

FDA, Food and Drug Administration; TGF- β , transforming growth factor- β ; ECM, extracellular matrix; α -SMA, α -smooth muscle actin; p.o., per os; VEGFR, Vascular Endothelial Growth Factor Receptor 2; FGFR, Fibroblast growth factor receptor-3; PDGFR, Platelet-derived growth factor receptor; LOXL2, lysyl oxidase-like 2; rt, room temperature; DMF, N, N-Dimethylformamide; TBAB, tetrabutylammonium bromide; TMS, Tetramethylsilane; SAR, structure-activity relationship; MTT, 3-(4,5-dimethylthiazol-2-yl)-2,5-diphenyltetrazolium bromide; SD, Standard Deviation; IC₅₀, Inhibitory concentration 50; TLC, thin-layer chromatography; UV, ultraviolet; NMR, nuclear magnetic resonance; MS (ESI), electrospray ionization mass spectrometry; DMSO, Dimethyl sulfoxide; ITS, Insulin-Transferrin-Selenium; PVDF, polyvinylidene fluoride; PK, pharmacokinetics.

Acknowledgment

The authors greatly appreciate the financial support from Drug Innovation Major Project (2018ZX09721002-001-004), National Natural Science (81874297) and 1.3.5 project for disciplines of excellence (ZY2017202) , West China Hospital, Sichuan University.

Reference

- [1] L. David, M. Fernando. Idiopathic Pulmonary Fibrosis. N. Engl. J. Med. 379 (2018) 797-798.
- [2] D Cécile, M. Toby. Recent advances in understanding idiopathic pulmonary fibrosis. F1000Res. 5 (2016).
- [3] Z.L. Wang. Advances in understanding of idiopathic pulmonary fibrosis. Chin Med J. 122 (2009) 844-857.
- [4] R. Luca, H.R. Collard, M.G. Jones. Idiopathic pulmonary fibrosis. Lancet. 389 (2017) 1941-1952.
- [5] F.J. Martinez, M.D. Martinez, et al. Randomized trial of acetylcysteine in idiopathic pulmonary fibrosis. N. Engl. J. Med. 370 (2014) 2093-2101.
- [6] G. Raghu , K.J. Anstrom , T.E. King, et al. Prednisone, azathioprine, and N-acetylcysteine for pulmonary fibrosis. N. Engl. J. Med. 366 (2012) 1968–1977.
- [7] G. Raghu, K.K. Brown, W.Z. Bradford, et al. A placebo-controlled trial of interferon gamma-1b in patients with idiopathic pulmonary fibrosis. N. Engl. J. Med. 350 (2004) 125-133.
- [8] I. Noth, K.J. Anstrom, S.B. Calvert, et al. A placebo-controlled randomized trial of

- 1236 warfarin in idiopathic pulmonary fibrosis. *Am. J. Respir. Crit. Care Med.* 186 (2012)
1237 88-95.
- 1238 [9] B.G. Fulton, C.J. Ryerson. Managing comorbidities in idiopathic pulmonary
1239 fibrosis. *Int. J. Gen. Med.* 8 (2015) 309-318.
- 1240 [10] D.A. Zisman, M. Schwarz, K.J. Anstrom, et al. A controlled trial of sildenafil in
1241 advanced idiopathic pulmonary fibrosis. *N. Engl. J. Med.* 363 (2010) 620-628.
- 1242 [11] G.J. Roth, A. Heckel, F. Colbatzky, et al. Design, synthesis, and evaluation of
1243 indolinones as triple angiokinase inhibitors and the discovery of a highly specific
1244 6-methoxycarbonyl-substituted indolinone (BIBF 1120). *J. Med. Chem.* 52 (2009)
1245 4466-4480.
- 1246 [12] I.A. Dimitroulis. Nintedanib: a novel therapeutic approach for idiopathic
1247 pulmonary fibrosis. *Respir Care.* 59 (2014) 1450-1455.
- 1248 [13] L. Richeldi, R.M. Du Bois, G. Raghu, et al. Efficacy and safety of nintedanib in
1249 idiopathic pulmonary fibrosis. *N. Engl. J. Med.* 370 (2014) 2071-2082.
- 1250 [14] G.J. Roth, R. Binder, F. Colbatzky, et al. Nintedanib: from discovery to the clinic.
1251 *J. Med. Chem.* 58 (2015) 1053-1063.
- 1252 [15] T. Ogura, A. Azuma, Y. Inoue, et al. All-case post-marketing surveillance of 1371
1253 patients treated with pirfenidone for idiopathic pulmonary fibrosis. *Respir. Investig.*
1254 53 (2015) 232-241.
- 1255 [16] E.K. Talmadge, A. Pardo, M. Selman. Idiopathic Pulmonary fibrosis. *Lancet.* 378
1256 (2011) 1949-1961.
- 1257 [17] X.H. Li, C. Lu, S.W. Liu, et al. Synthesis and discovery of a drug candidate for

- 1258 treatment of idiopathic pulmonary fibrosis through inhibition of TGF- β 1 pathway. Eur
1259 J. Med. Chem. 157 (2018) 229-247.
- 1260 [18] R.E. Gilbert, Y. Zhang, S.J. Williams, et al. A purpose-synthesised anti-fibrotic
1261 agent attenuates experimental kidney diseases in the rat. PLOS ONE. 7, e47160.
- 1262 [19] D.X. Deng, H.Y. Pei, T.X. Lan, et al. Synthesis and discovery of new compounds
1263 bearing coumarin scaffold for the treatment of pulmonary fibrosis. Eur. J. Med. Chem.
1264 2019. <https://doi.org/10.1016/j.ejmech.2019.111790>.
- 1265 [20] I. Noth, K.J. Anstrom, S.B. Calvert, et al. Idiopathic pulmonary fibrosis clinical
1266 network (IPFnet). A placebo-controlled randomized trial of warfarin in idiopathic
1267 pulmonary fibrosis. Am. J. Respir. Crit. Care. Med. 186 (2012) 88–95.
- 1268 [21] L Sun, Ngoc Tran, C X Liang, et al. Design, synthesis, and evaluations of
1269 substituted 3-[(3- or 4-Carboxyethylpyrrol-2-yl)methylidenyl]indolin-2-ones as
1270 Inhibitors of VEGF, FGF, and PDGF receptor tyrosine kinases. J. Med. Chem. 42
1271 (1999) 5120-5130.
- 1272 [22] G.A. Freeman, C.W. Andrews III, A.L. Hopkins, et al. Design of Non-nucleoside
1273 Inhibitors of HIV-1 Reverse Transcriptase with Improved Drug Resistance Properties.
1274 J. Med. Chem. 47 (2004) 5923-5936.
- 1275 [23] N. Brown. Bioisosteres and scaffold hopping in medicinal chemistry. Mol.
1276 Inform. 33 (2014) 458-462.
- 1277 [24] Q. Xu, J.T. Norman, S. Shrivastav, et al. In vitro models of TGF-beta-induced
1278 fibrosis suitable for high-throughput screening of antifibrotic agents. AJP: Renal
1279 Physiology. 293 (2007) F631-F640.

- 1280 [25] H.B. Xiao, R.H. Liu, G.H. Ling, et al. HSP47 regulates ECM accumulation in
1281 renal proximal tubular cells induced by TGF-beta1 through ERK1/2 and JNK MAPK
1282 pathways. *Am. J. Physiol. Renal. Physiol.* 303 (2012) F757-F765.
- 1283 [26] J.F. Dhainaut, J. Charpentier, J.D. Chiche. Transforming growth factor-beta: a
1284 mediator of cell regulation in acute respiratory distress syndrome. *Crit Care Med.* 31
1285 (2003) S258-264.
- 1286 [27] I.A. Darby, O. Skalli, G. Gabbiani. Alpha-smooth muscle actin is transiently
1287 expressed by myofibroblasts during experimental wound healing. *Lab. Invest.* 63
1288 (1990) 21-29.
- 1289 [28] G. Gabbiani. The myofibroblast in wound healing and fibro contractive diseases.
1290 *J. Pathol.* 200 (2003) 500-503.
- 1291 [29] N. Venkatesan, L. Pini, M.S. Ludwig. Changes in Smad expression and
1292 subcellular localization in bleomycin-induced pulmonary fibrosis. *Am. J. Physiol.*
1293 *Lung Cell Mol. Physiol.* 287 (2004) L1342-1347.
- 1294 [30] T. Hayashida, M. Decaestecker, H.W. Schnaper. Cross-talk between ERK MAP
1295 kinase and Smad signaling pathways enhances TGF-beta-dependent responses in
1296 human mesangial cells. *FASEB J.* 17 (2003) 1576-1578.
- 1297 [31] N.A. Bhowmick, R. Zent, M. Ghiassi, et al. Integrin beta 1 signaling is necessary
1298 for transforming growth factor-beta activation of p38 MAPK and epithelial plasticity.
1299 *J. Biol. Chem.* 276 (2001) 46707-46713.
- 1300 [32] T. Hayashida, M.H. Wu, A. Pierce, et al. MAP-kinase activity necessary for
1301 TGF-beta1-stimulated mesangial cell type I collagen expression requires

- 1302 adhesion-dependent phosphorylation of FAK tyrosine 397. J. Cell. Sci. 120 (2007)
1303 4230-4240.

Highlights

- Hybridization of 2(1H)-quinolone skeleton and hydrophobic group of nintedanib.
- Successful application of bioisosteres reduced toxicity of compounds.
- Anti-fibrosis by inhibiting TGF- β /Smad dependent and independent pathways.
- Excellent anti-fibrotic effect under both prevention and treatment model *in vivo*.

Declaration of Interest Statement

We declare that we have no financial and personal relationships with other people or organizations that can inappropriately influence our work.

Journal Pre-proof